The effect of *Cyp3a* deficiency on the hepatic cholesterol synthesis and prostatic androgen response in the mouse

Cytochrome P450 3A 欠損マウスにおける肝コレステロール合成および
前立腺アンドロゲン応答の亢進

2016年

分子薬物治療学講座（薬物学研究室）

橋本真里

Abbreviations

Androgen receptor	AR
Androgen response element	ARE
ATP-binding cassette	ABC
Chromatin immunoprecipitation	ChIP
Cytochrome P450	CYP
D-dopachrome tautomerase	DDT
Dihydrotestosterone	DHT
Farnesoid X receptor	FXR
HMG-CoA reductase	HMGCR
HMG-CoA synthase 1	HMGCS1
25-Hydroxycholesterol	25HC
6β-Hydroxytestosterone	6βHT
7α-Hydroxy-4-cholesten-3-one	C4
Knockout	KO
Low-density lipoprotein receptor	LDLR
Liver X receptor α	LXRα
Multidrug resistance 1a	Mdr1a
Niemann-Pick C1-like 1	NPC1L1
Organic anion transporting polypeptide 2	OATP2
Phosphate buffered saline	PBS
Pregnane X receptor	PXR
Proliferator-activated receptor γ coactivator-1α	PGC1α
Protein kinase C delta	PRKCD
Sex hormone–binding globulin	SHBG
Small heterodimer partner	SHP
Spermine-binding protein	SBP
Squalene epoxidase	SQLE
SREBP cleavage-activating protein	SCAP
Steroid 5α-reductase 2	SRD5A2
Sterol regulatory element binding protein 2	SREBP2
Sterol regulatory element-binding factor 2	SREBF2
Sterol response element	SRE
Sulfotransferase 2a1	SULT2A1
TATA-binding protein	TBP
Wild type	WT

Contents

Introduction

CYP3A subfamily consists of four and six isoforms in human and mouse, respectively. CYP3A isoforms are abundantly expressed in the liver and small intestine which are critical tissues for drug metabolism. More than 50% of clinically used drugs are metabolized by CYP3A. Thus, CYP3A is the most important cytochrome P450 isoforms responsible for drug metabolism [1]. In addition, CYP3A catalyzes hydroxylation of endogenous compounds such as bile acids, steroid hormones and vitamins [2-5]. For example, cholesterol and testosterone are metabolized by CYP3A to their inactive forms, 25-hydroxycholesterol (25HC) and 6β-hydroxytestosterone (6βHT), respectively, in both human and mouse [6-7]. Thus, CYP3A may play some role in the regulation of physiological levels of endogenous compounds in the body.

Cholesterol is one of components of cellular membrane, which is supplied from endogenous synthesis and diet. A master regulator of cholesterol homeostasis is sterol regulatory element binding protein 2 (SREBP2) which regulates synthesis and uptake of cholesterol [8]. When cellular cholesterol levels are decreased, SREBP cleavage-activating protein (SCAP) escorts SREBP2 from endoplasmic reticulum membrane to Golgi body where SREBP2 is processed to an active form [8]. The activated SREBP2 translocates to nucleus, and activates transcription of genes involved in synthesis and uptake of cholesterol [8]. On the other hand, under the high cholesterol condition, formation rate of 25HC is increased, and increased 25HC effectively suppresses activation of SREBP2 by disturbing disengagement of SREBP2 from endoplasmic reticulum membrane, which leads suppression of cholesterol synthesis and uptake [9]. Thus, the formation of 25HC by CYP3A is considered to be a feedback mechanism which is responsible for the maintenance of cholesterol homeostasis. However, not only CYP3A but also cholesterol 25-hydroxylase, CYP27A1 and auto-oxidation are involved in the formation of 25HC [10-13]. Therefore, the physiological role of CYP3A as an enzyme catalyzing cholesterol 25-hydroxylation to maintain cholesterol homeostasis remains obscure, and the possibility that 25-hydroxylation of cholesterol by CYP3A is involved in the regulation of synthesis and uptake of cholesterol in liver should be examined.

Testosterone is a major androgen in human plasma. Testosterone provided from systemic circulation contributes to development and functions of prostate through activation of androgen receptor (AR) [14]. In addition, androgen enhances cholesterol synthesis in prostate by the following mechanism. Prostatic AR activated by androgen increases expression levels of SCAP, which sequentially enhances cholesterol synthesis through SREBP2 activation [15, 16]. On the other hand, circulating testosterone is mainly converted to inactive form in liver [17]. Since CYP3A metabolizes testosterone into 6βHT which has negligible potency to activate AR, hepatic CYP3A is considered to

contribute to the inactivation of testosterone in the body [17, 18]. However, to what extent CYP3A contributes to the overall inactivation of testosterone in the body remains to be clarified. In addition, whether alteration of CYP3A activity affects cholesterol synthesis via AR-SCAP-SREBP pathway in prostate also remains to be clarified.

The generation of gene knockout mice has provided a useful tool in understanding the gene function. Previously, van Herwaarden *et al* have shown the effect of *Cyp3a* deficiency on detoxification of docetaxel using *Cyp3a* knockout mice [19]. However, the effect of *Cyp3a* deficiency on physiological functions of *Cyp3a* has not been elucidated. Therefore, the purpose of this study is to clarify the potential role of *Cyp3a* in cholesterol synthesis in liver and prostate. In the chapter 1, the effect of *Cyp3a* deficiency on cholesterol synthesis, and its effect on bile acid synthesis which is initiated from cholesterol hydroxylation, were investigated using *Cyp3a*$^{-/-}$ mice. In the chapter 2, the effect of *Cyp3a* deficiency on testosterone levels in plasma, and cholesterol synthesis in prostates were investigated using *Cyp3a*$^{-/-}$ mice.

Chapter Ⅰ

Studies on the effects of *Cyp3a* deficiency on cholesterol and bile acid synthesis in liver

1-1. Introduction

Cholesterol has multifunctional roles as components of cellular membranes and precursors of biological molecules such as steroid hormones, oxysterols, vitamins and bile acids in humans and animals [20-23]. The endogenous synthesis of cholesterol is catalyzed by many enzymes including HMG-CoA synthase 1 (HMGCS1), HMG-CoA reductase (HMGCR) and squalene epoxidase (SQLE). When cellular sterol levels are low, SREBP2 is processed by proteases and translocates into the nucleus. Nuclear SREBP2 activates the transcription of genes encoding enzymes involved in the biosynthesis of cholesterol [24]. Thus, SREBP2 is considered as a master regulator of cholesterol biosynthesis [8].

Hepatic cholesterol levels are regulated by elaborate networks such as influx, efflux, and conversion into bile acids in addition to biosynthesis. Dietary cholesterol is absorbed from the jejunum and transported to the liver [25]. A part of cholesterol in the liver is enclosed in lipoprotein and excreted into blood circulation. Hepatic cholesterol is also secreted into the duodenum *via* the biliary canaliculus. Most of the biliary cholesterol is reabsorbed in the jejunum with dietary cholesterol and transported back to the liver [25]. Such behavior of cholesterol is regulated by many transporters. For example, Niemann-Pick C1-like 1 (NPC1L1) imports cholesterol from the lumen into enterocytes of the intestine [26]. At the basolateral membrane of the intestine, ATP-binding cassette (ABC) A1 transports cholesterol into the bloodstream. In the liver, ABCA1 also functions at basolateral surface to transport cholesterol into the bloodstream [27]. ABCG5 and ABCG8 form a functional heterodimer complex that mediates the secretion of cholesterol from hepatocytes into the biliary canaliculus and also the apical efflux of cholesterol from enterocytes into the lumen of the intestine [28, 29]. Hepatic low-density lipoprotein receptor (LDLR) is responsible for uptake of LDL cholesterol from blood circulation into hepatocytes [30]. On the other hand, a part of cholesterol in the liver is metabolized to bile acids through many steps catalyzed by enzymes such as CYP7A1 and CYP8B1 [31]. Bile acids are excreted into the biliary canaliculus with cholesterol and then assist the absorption of biliary and dietary cholesterol in the intestine.

Members of the CYP3A subfamily are the most abundant CYP enzymes in the liver and small intestine. CYP3A enzymes metabolize over 50% of drugs in clinical use and are therefore closely involved in pharmacokinetics, drug interactions, drug efficacy and toxicity [1]. CYP3A enzymes metabolize not only xenobiotics but also many endogenous compounds such as cholesterol, bile acids, steroid hormones and vitamins. The extremely wide substrate specificity of CYP3A enzymes has resulted in versatile physiological functions of CYP3A [2-5]. As for cholesterol, it has been reported that human CYP3A4 mediates the conversion of cholesterol into 4β-HC, an endogenous oxysterol [32, 33]. 4β-HC is expected to be useful as an endogenous marker of CYP3A because it is found in human circulation [5]. In addition, a recent study demonstrated that CYP3A was involved in 25-hydroxylation of cholesterol [6]. 25-HC acts as not only a precursor of bile acids but also a physiologically active oxysterol that suppresses SREBP2 and down-regulates cholesterol biosynthesis [9, 34, 35]. However, the roles of cholesterol metabolites formed by CYP3A in biosynthesis of cholesterol have not been fully elucidated, particularly in *in vivo* experiments.

The *Cyp3a*-knockout (*Cyp3a*$^{-/-}$) mouse is a valuable research tool in studies on drug metabolism and drug-induced toxicity *in vivo* [19, 36]. However, the physiological role of CYP3A has not been clearly elucidated in *in vivo* experiments. To reveal the role of CYP3A in cholesterol homeostasis, we investigated the effects of CYP3A deficiency on expression levels of genes responsible for influx, efflux, metabolism and biosynthesis of cholesterol using *Cyp3a*$^{-/-}$ mice.

1-2. Materials and Methods

1-2-1. Chemicals

7α-Hydroxy-4-cholesten-3-one (C4) was purchased from Santa Cruz (Santa Cruz, CA). 25HC was purchased from Steraloids (Newport, RI). Lathosterol was purchased from Sigma-Aldrich (St. Louis, MO). Acetonitrile, chloroform, hexane and methanol were HPLC grade (Wako, Tokyo, Japan).

1-2-2. Animals

C57BL/6JJcl mice (CLEA, Tokyo, Japan) were used as wild type (WT) mice. Recently, we generated *Cyp3a*$^{-/-}$ mice by targeted deletion of endogenous *Cyp3a* genes [37]. Brief, *Cyp3a13*$^{-/-}$ lines and *Cyp3a57-59*$^{-/-}$ lines were generated by conventional gene targeting and Cre-loxP mediated chromosomal deletion, respectively, and the two lines were mated to generate *Cyp3a*$^{-/-}$ mice lacking the mouse *Cyp3a* gene cluster. The distance between the *Cyp3a57-59* gene cluster and a *Cyp3a13*$^{-/-}$ gene is ~5 Mb and several genes are located between the loci, so the two knockout lines were generated independently. It has been confirmed that the six genes on the mouse *Cyp3a* cluster (*Cyp3a13/57/44/11/25/59*) were expressed in the livers and intestines of WT mice but not in those of *Cyp3a*$^{-/-}$ mice [37]. Fetal specific *Cyp3a16* and female specific *Cyp3a41* were not detected at mRNA levels because only adult male mice were used in this study (data not shown). In addition, α- and 4-hydroxylation activities of triazolam, which are catalyzed by mouse CYP3A [38], in the liver microsomes of *Cyp3a*$^{-/-}$ mice were less than 7% of those in WT mice (Fig. 1). These findings suggest the complete deletion of CYP3A functions in *Cyp3a*$^{-/-}$ mice used in the present study. The control genetic background is almost same as *Cyp3a*$^{-/-}$ mice, because *Cyp3a*$^{-/-}$ mice were backcrossed to C57BL/6JJcl mice at least 4 times. All experiments were done using male mice between 10 and 11 weeks of age. Animals were kept in a temperature-controlled environment with a 12-hr light/dark cycle. The light-cycle hours were between 7 AM and 7 PM. They received a standard diet containing 0.1% cholesterol (CE-2, CLEA, Tokyo, Japan, Table 1). Animals were sacrificed between 10 AM and 11 AM without fast. The present study was conducted in accordance with the guidelines for the Care and Use of Laboratory Animals, as adopted by the Committee on Animal Research of Tottori University and Chiba University.

1-2-3. RNA isolation and cDNA synthesis

Total RNA was isolated from tissue pieces of livers and small intestines. Since most of cholesterol is reabsorbed in jejunum [25], the upper parts of small intestines (1-cm segments collected at 10 cm from the pyloric region) were used. Total RNA was extracted by using ISOGEN (Nippon Gene, Tokyo, Japan) and was purified using RNeasy columns (Qiagen, Hilden, Germany) were used

in accordance with the manufacturer's instructions, and then treated with RNase-free DNase I (Wako Pure Chemicals, Osaka, Japan). The cDNA was generated with a random hexamer by using a High-Capacity cDNA Reverse Transcription Kit (Applied Biosytems, Foster, CA).

1-2-4. Analysis of mRNA levels

Expression levels were measured by quantitative real-time PCR carried out on an EcoReal-time PCR system (Illumina, Hayward, CA). Expression levels of HMGCS1, HMGCR, SQLE, sterol regulatory element-binding factor 2 (SREBF2), ABCG5, ABCG8, ABCA1, LDLR, NPC1L1, CYP7A1, CYP8B1, CYP27A1, CYP7B1 and small heterodimer partner (SHP), organic anion transporting polypeptide (OATP2) and sulfotransferase 2a1 (SULT2A1) were measured by SYBR Green based real-time PCR using KAPA SYBR Fast ABI Prism 1000 (KAPA Biosystems, Woburn, MA). Specific primers for real-time PCR are presented in Table 2. Expression levels of CYP2C55, CYP2B10 and multidrug resistance 1a (Mdr1a) mRNA were measured using TaqMan Gene Expression Assays. (Mm00472168_m1, Mm00456591_m1 and Mm00440761_m1, Applied Biosystems). The expression levels of mRNA were normalized with the expression level of mouse GAPDH as an endogenous control gene.

1-2-5. Preparation of nuclear extracts

Nuclear fractions were prepared from liver tissues. Aliquots of frozen liver (about 100 mg) were homogenized in 1 ml of lysis buffer (10 mM HEPES adjusted to pH 7.9, 1.5 mM $MgCl_2$ and 10 mM KCl) supplemented with protease inhibitor cocktail set III (Calbiochem, La Jolla, CA) and 1 mM DTT. The liver homogenate was centrifuged at 10,000 × *g* for 5 min at 4°C. The supernatant (cytosol fraction) was removed and stored at -80°C. The nuclear pellet was resuspended in 0.15 ml extraction buffer (20 mM HEPES adjusted to pH 7.9, 2.5% glycerol, 0.42 M NaCl and 1.5 mM $MgCl_2$) supplemented 1 mM DTT and protease inhibitor cocktail set III. The suspension was rotated at 4°C for 30 min and centrifuged at 20,000 × *g* for 15 min at 4°C. The supernatant from this spin was designated as the nuclear extract and stored at -80°C until use.

1-2-6. Western blot analysis

Nuclear extracts (30 μg/lane) were separated by 10% SDS-polyacrylamide gel electrophoresis and transferred to a nitrocellulose membrane. After 1-hr incubation with blocking buffer (0.05% Tween 20 in PBS containing 3% skim milk), the membrane was probed for 1 hr at room temperature using a polyclonal anti-SREBP2 rabbit antibody (1:500 dilution, Ab2848, Abcam, Cambridge, UK). A monoclonal anti-TATA-binding protein (TBP) mouse antibody (1:2000 dilution, Ab818, Abcam) was used as an internal control. After washing, the membrane was incubated with a peroxidase-

conjugated secondary antibody for 1 hr at room temperature. The secondary antibodies used were anti-rabbit IgG (1:100,000 dilution, Sigma-Aldrich) and anti-mouse IgG (1:5000 dilution, Sigma-Aldrich) for anti-SREBP2 and anti-TBP antibodies, respectively. The primary and secondary antibodies were diluted with 0.05% Tween 20 in PBS containing 3% BSA. Protein bands were visualized by using an ECL Western Blotting Detection Reagents (GE Healthcare, Buckingham, UK), ImmunoStar LD (Wako) and LAS-1000 plus (Fujifilm, Tokyo, Japan).

1-2-7. Chromatin immunoprecipitation (ChIP) assay

Liver tissue (100 mg) of WT and *Cyp3a*$^{-/-}$ mice was minced and formaldehyde was added to a final concentration of 1%. After rocking at room temperature for 15 min, glycine was added to a final concentration of 0.125 M to stop the cross-linking. The tissues were collected by centrifugation and were homogenized by a dounce homogenizer in cold cell lysis buffer (5 mM PIPES, pH 8.0, 85 mM KCl, 0.5% Nonidet P-40) supplemented with proteinase inhibitor cocktail set III (Calbiochem). Nuclei pellets were collected by centrifugation at 6,200 × *g* for 10 min at 4°C and resuspended in 400 µl of nuclei lysis buffer (50 mM Tris-HCl, pH 8.1, 10 mM EDTA, 1% SDS) supplemented with proteinase inhibitor cocktail set III (Calbiochem). Nuclei were sonicated before immunoprecipitation with polyclonal anti-SREBP2 rabbit antibody (ab28482, Abcam) or normal IgG (sc2027, Santa Cruz, CA) overnight at 4°C. DNA in the precipitated samples was reverse cross-linked at 65°C for 6 hr, and the DNA was recovered by phenol/chloroform extraction and ethanol precipitation. DNA samples were measured by semi-quantitative PCR with Go Taq® Green Mater Mix (Promega, Madison, WI) and quantitative PCR using SYBR Green based real-time PCR with KAPA SYBR Fast ABI Prism 1000 (KAPA Biosystems). PCR was carried out with *Hmgcs1*-specific primers encompassing the sterol regulatory elements (SRE) site in the 5'-flanking region (-348 to -208 bp) and a region in intron 5 (+11862 to +11948 bp) as a negative control. The PCR conditions were one cycle of pre-denaturation at 95°C for 10 min, 45 cycles of denaturation at 95°C for 15 sec, annealing at 58°C for 30 sec, and elongation at 72°C for 15 sec. The primers used are as follows: *Hmgcs1/*SRE, 5'-ATTGGTCGGAGAACCTCTC-3' and 5'-AGGGGTGGGAACAAAGTCC-3': *Hmgcs1*/negative control, 5'-ATTAGACAGGATTTGGGGTCACT-3' and 5'-GTCTACACTGCAAAGAGAGCAGG-3'.

1-2-8. Cholesterol analysis

Hepatic lipids were extracted according to the procedure of Bligh and Dyer [39] with slight modification. Briefly, frozen liver tissues (about 5 mg) were homogenized and extracted with a mixture of chloroform/isopropanol/Triton X-100 (7:11:0.1, v/v/v). The organic layer was subjected to cholesterol determination after evaporation and resuspension in methanol. Total cholesterols in liver and plasma were determined by use of a Cholesterol E-Test Wako kit (Wako) according to the

manufacturer's instructions.

1-2-9. Analysis of plasma lathosterol

Concentration of lathosterol in plasma was determined by an HPLC method. To extract lipids, plasma (0.1 ml) was diluted with 0.1 ml of distilled water and vigorously mixed with 0.8 ml of hexane for 1 min, and then centrifuged at 2000 × g for 5 min. The supernatant (hexane layer) was transferred to a new tube and further extracted once with 0.2 ml of water. Separately the water layer was further extracted twice with 0.8 ml of hexane. The hexane extracts were combined, and dried under vacuum. The residue was reconstituted with 0.1 ml of methanol, and 50 μl of 15 reconstituted sample was injected onto a Hitachi L-7000 model of HPLC system (Tokyo, Japan) and Poroshell120 EC-C18 (3.0 × 100 mm, 2.7 μm) column (Agilent technology, Santa Clara, CA). The mobile phase consisted of acetonitrile/methanol (8:2, v/v) at a flow rate of 0.6 ml/min. The eluent was monitored at a wavelength of 235 nm.

1-2-10. Analysis of 25HC in the liver

Concentration of 25HC in the liver was determined by methods described elsewhere [6] with slight modifications. In brief, liver tissues (50 mg) were homogenized in 0.1 M potassium phosphate buffer (pH 7.4) containing 4 mM $MgCl_2$, 1 mM EDTA and 30 mM nicotinamide. The homogenates were incubated with 1 N ethanolic potassium hydroxide, extracted with hexane and derivatized to picolinyl esters. The samples were analyzed by HPLC-MS/MS using Triple TDF^{TM} 5600 System (AB SCIEX, Framingham, MA).

1-2-11. Analyses of total bile acids and their intermediary product C4

Bile acid levels in the liver were determined following bile acid extraction of liver tissues. Briefly, liver tissues (200 mg) were homogenized in 1 ml of ethanol and heated at 85°C for 1 min and then centrifuged at 1000 × g for 5 min. After the supernatant was isolated, the precipitate was extracted twice with 1 ml of ethanol and the combined extracts were dried under vacuum. The residue was resuspended in 0.2 ml of 75% methanol and centrifuged at 14,000 × g for 10 min, filtered using a filter unit (0.45 μm, Millipore, Billerica, MA) and dried under vacuum. The residue was reconstituted with 10 μl of 75% methanol. After dilution with distilled water, the sample was analyzed by use of total bile-Test Wako kit (Wako) according to the manufacturer's instructions. Size of bile acid pool was expressed as sum of total bile acid content in the liver, small intestine and gallbladder per 100 g body weight. Bile acid content in small intestine was determined after extraction of small intestine tissues (200 mg) as described for bile acid content in the liver. For gallbladder, bile drawn from gallbladder was diluted with distilled water of 2 ml/mg tissue of empty gallbladder and analyzed as described

above. Concentration of C4, an intermediary product in the synthesis of bile acids, in plasma was determined by an HPLC method of Lenicek et al. [40] with slight modifications. Plasma (0.2 ml) was vigorously mixed with 2.5 ml of chloroform/methanol (2:1, v/v), and centrifuged at 2000 × g for 3 min. After the upper phase was discarded, the lower phase was mixed with 1 ml of 125 mM NaCl in 50% methanol, and centrifuged as above. The lower phase was dried under vacuum. The residue was reconstituted with 0.2 ml of acetonitrile. Eighty μl of reconstituted sample was injected onto a Hitachi L-7000 model of HPLC system and a CAPCELL PAK C18 UG120 column (4.6 mm × 250 mm, 5 μm; Shiseido, Tokyo, Japan). The mobile phase consisted of acetonitrile/water (92:8, v/v) at a flow rate of 1.0 ml/min. The eluent was monitored at a wavelength of 241 nm.

1-2-12. Statistical analysis

Number of mice in each group was described in legends of figures and tables. Data are shown as means ± S. E. M. or S. D. Statistical analyses were performed by using Statcel (OMS, Saitama, Japan). Comparison was made with Student's *t*-test or Welche's *t*-test. $P < 0.05$ was considered statistically significant.

Table 1. Nutrient composition of CE-2 diet

Nutrient	Composition
Moisture (%)	8.9
Crude protein (%)	24.9
Crude fat (%)	4.6
Crude fiber (%)	4.1
Crude ash (%)	6.6
Nitrogen-free extract (%)	51.0
Energy (kcal/g)[a]	3.4

Note. Values and nutrients are provided in the catalog of CLEA Japan Inc.(2013).
[a]Physiological fuel value with no caloric value for crude fiber.

Table 2. Sequences of primers used in real-time PCR

Gene	Forward Primer (5’ to 3’)	Reverse Primer (5’ to 3’)
Hmgcs1	TGGCACAGTACTCACCTC	CCTTCATCCAAACTGTGG
Hmgcr	CTTGTGGAATGCCTTGTGATTG	AGCCGAAGCAGCACATGAT
Sqle	AAATCAGAGCCGTGGGCTAC	GGAAGTGACACAGTTCTATG
Srebf2	GGTCCTCCATCAACGACAA	CTCAGAACGCCAGACTTGTGC
Abcg5	ATCGCAGCCCAACTCCTTCAG	CAGTCCAGTCCTGTGGTTGGC
Abcg8	GCCACCCTTGTCCTCGCTA	TTCTTTGCTGCGTCTGTCGAT
Abca1	GATGTGGAATCGTCCCTCAGTTC	ACTGCTCTGAGAAACACTGTCCTCC
Ldlr	GTGCATGGCTTCATGTAC	TCATAGATGGCCAAGGAG
Npc1l1	TCTACTGTGCCAATGCCCCTCTC	CCCGTAGTCAGCTATGCAGCTCA
Cyp7a1	AGCAACTAAACAACCTGCCAGTACTA	GTCCGGATATTCAAGGATGCA
Cyp8b1	GAAGATCCACCACTACAGCAT	GGACAAAGGTCTTCATCTCG
Cyp27a1	CCAGGCACAGGAGAGTACG	GGGCAAGTGCAGCACATAG
Cyp7b1	GAAAACTCTTCAAAGGCAACATGG	ACTGGAAAGGGTTCAGAACAAATG
Shp	TTCAACCCAGATGTGCCAGG	CAAATGCTCCTGTTGCAGGTGTGCGA
Oatp2	ATTCGTGAGTTACTTCGGAACA	CCCATAACTGCACATCCTACAC
Sult2a1	CCTCCCATCTTCCCATCCAT	CTCACGAGATAGATCGCCTTGG
Gapdh	TGCACCACCAACTGCTTA	GGATGCAGGGATGATGTTC

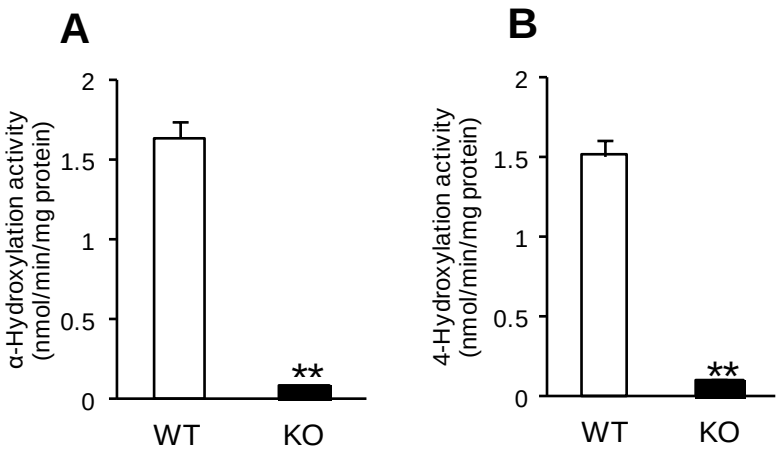

Fig. 1. α-Hydroxylation (A) and 4-hydroxylation (B) activities of triazolam in liver microsomes of WT and *Cyp3a*$^{-/-}$ (KO) mice.

Triazolam (200 μM) was incubated with liver microsomes of WT and KO mice as described in elsewhere (27). Data are shown as means ± S. E. M. of three mice in each group. Liver microsomes prepared from each mouse were used for three independent determinations, each performed in duplicate. ***P* < 0.01 versus WT mice.

1-3. Results

1-3-1. Effects of CYP3A deficiency on expression levels of enzymes involved in cholesterol biosynthesis

We measured the mRNA levels of HMGCS1, HMGCR and SQLE in the livers of WT and *Cyp3a*$^{-/-}$ mice in order to investigate the effects of CYP3A deficiency on mRNA expression of enzymes involved in cholesterol biosynthesis. As shown in Fig. 2, expression levels of HMGCS1 and SQLE mRNAs in the livers of *Cyp3a*$^{-/-}$ mice were significantly higher than those of WT mice (5.4 and 4.9 fold, respectively). Expression levels of HMGCR mRNAs in the livers of *Cyp3a*$^{-/-}$ mice showed a trend toward higher levels than those of WT mice, although the differences were not significant. Expression levels of HMGCS1 and SQLE mRNAs in the small intestine were similar between WT and *Cyp3a*$^{-/-}$ mice. Expression levels of HMGCR mRNAs in the small intestines of *Cyp3a*$^{-/-}$ mice were 1.4-fold higher than those of WT mice (Fig. 3).

1-3-2. Effects of CYP3A deficiency on expression of SREBP2

The *Srebf2* gene encoding SREBP2 is also known as a target gene of SREBP2 [8]. As shown in Fig. 4A, expression levels of SREBF2 mRNA in the livers of *Cyp3a*$^{-/-}$ mice were 1.9-fold higher than those of WT mice ($P < 0.001$). In the small intestine, expression levels of SREBF2 mRNAs were similar between WT and *Cyp3a*$^{-/-}$ mice (Fig. 3). Since mRNA expression levels of HMGCS1, SQLE and SREBF2 in the livers of *Cyp3a*$^{-/-}$ mice were significantly higher than those of WT mice, we determined nuclear levels of SREBP2 protein in the livers of WT and *Cyp3a*$^{-/-}$ mice. As shown in Fig. 4B, nuclear levels of SREBP2 protein in the livers of *Cyp3a*$^{-/-}$ mice were markedly higher than those in WT mice.

1-3-3. Effects of CYP3A deficiency on SREBP2 binding to the SRE motif

To verify whether CYP3A deficiency affected binding of SREBP2 to an SRE motif in a genomic context, ChIP assays were performed with livers of WT and *Cyp3a*$^{-/-}$ mice. The *Hmgcs1* promoter contains a known SRE motif [41]. The specific binding of SREBP2 to the SRE-containing region (-348 to -208 bp) was significantly more abundant in the livers of *Cyp3a*$^{-/-}$ mice than in the livers of WT mice ($P < 0.01$, Fig. 5). The degree of binding of SREBP2 to the negative control region was low and showed no difference between WT and *Cyp3a*$^{-/-}$ mice.

1-3-4. Effects of CYP3A deficiency on cholesterol biosynthesis

Since transcription of genes encoding enzymes involved in cholesterol biosynthesis enhanced

in *Cyp3a*$^{-/-}$ mice, we examined total cholesterol levels in the plasma and livers, lathosterol levels in the plasma and 25-HC levels in the livers of WT and *Cyp3a*$^{-/-}$ mice. As shown in Table 3, body weight and liver weight of *Cyp3a*$^{-/-}$ mice were higher than those of WT mice. Total cholesterol levels in the livers of *Cyp3a*$^{-/-}$ mice were about 20% lower than those in the livers of WT mice ($P < 0.05$), although no significant difference was found in plasma total cholesterol levels between WT and *Cyp3a*$^{-/-}$ mice. Plasma lathosterol levels, as an indicator of cholesterol biosynthesis [42], showed a trend toward higher than those of WT mice, although the difference was not significant. 25-HC levels in the livers of *Cyp3a*$^{-/-}$ mice were significantly lower than those in the livers of WT mice ($P < 0.05$).

1-3-5. Effects of CYP3A deficiency on expression levels of cholesterol transporters

To investigate the mechanism of decreased hepatic total cholesterol in *Cyp3a*$^{-/-}$ mice, we determined the mRNA expression levels of genes involved in the influx and efflux of cholesterol. As shown in Fig. 6A, no significant differences in expression levels of ABCG5, ABCG8, ABCA1 and LDLR mRNAs in the liver were found between WT and *Cyp3a*$^{-/-}$ mice. As shown in Fig. 6B, expression levels of ABCG5, ABCG8 and ABCA1 mRNAs in the small intestine were also similar between WT and *Cyp3a*$^{-/-}$ mice. Expression levels of NPC1L1 mRNA in the small intestines of *Cyp3a*$^{-/-}$ mice were 1.7-fold higher than those of WT mice.

1-3-6. Effects of CYP3A deficiency on bile acid biosynthesis

Synthesis and secretion of bile acids constitute a major route for elimination of cholesterol from the liver [31]. To determine the mechanism of reduction of hepatic cholesterol in *Cyp3a*$^{-/-}$ mice, we investigated expression levels of four enzymes involved in bile acid biosynthesis. The classical pathway of bile acid synthesis is initiated by 7α-hydroxylation of cholesterol catalyzed by CYP7A1, which is a rate-limiting enzyme of this pathway [31]. The next product C4 is metabolized to 7α, 12α-dihydroxy-4-cholesten-3-one by CYP8B1. Then the resulting product is converted ultimately into bile acid [31]. An alternative pathway of bile acid synthesis is initiated by 27-hydroxylation of cholesterol catalyzed by CYP27A1 [31]. Subsequently, 27-HC is metabolized to 7α, 27-diHC by CYP7B1 and 3β-hydroxy-5-cholestenoic acid by CYP27A1 [31]. As shown in Fig. 7, the expression levels of CYP7A1, CYP8B1 and CYP7B1 mRNAs were significantly higher in the livers of *Cyp3a*$^{-/-}$ mice than those of WT mice (1.9, 2.7 and 3.3 fold, respectively). Expression levels of CYP27A1 and SHP mRNAs in the liver were similar between WT and *Cyp3a*$^{-/-}$ mice.

Since the expression levels of CYP7A1, CYP8B1 and CYP7B1 were higher in the livers of *Cyp3a*$^{-/-}$ mice compared with WT mice, we studied whether bile acid synthesis was enhanced in *Cyp3a*$^{-/-}$ mice. As shown in Fig. 8A, plasma concentration of C4 was 1.6-fold higher in *Cyp3a*$^{-/-}$ mice than in WT mice ($P < 0.05$). As shown in Fig. 8B, total bile acid levels in the livers of *Cyp3a*$^{-/-}$ mice were also significantly higher than those of WT mice ($P < 0.05$). Bile acid pool size of *Cyp3a*$^{-/-}$ mice showed a

trend toward higher levels than those of WT mice, although differences were not significant (Fig. 8C).

1-3-7. Effects of CYP3A deficiency on expression of target genes of PXR

Since activated pregnane X receptor (PXR) could suppress transcription of mouse *Cyp7a1* gene [43, 44], we measured the mRNA expression levels of target genes of PXR in the livers of WT and *Cyp3a*$^{-/-}$ mice. The mRNA expression levels of Mdr1a in the livers of *Cyp3a*$^{-/-}$ mice were lower than those of WT mice, whereas expression levels of OATP2, SULT2A1, CYP2C55 and CYP2B10 mRNAs in the livers of *Cyp3a*$^{-/-}$ mice were higher than those of WT mice (Fig. 9).

Table 3. Body and liver weight, and plasma and hepatic levels of cholesterol and oxysterol in WT and *Cyp3a*$^{-/-}$ mice

	Genotype	
Parameter	WT	*Cyp3a*$^{-/-}$
Body weight (g)	23.7 ± 0.3	27.7 ± 1.1^{a}
Liver weight (g)	1.0 ± 0.03	1.5 ± 0.07^{b}
Plasma lathosterol (ng/mL)	32.1 ± 2.0	41.3 ± 7.9
Plasma total cholesterol (mg/dL)	63.4 ± 9.8	82.6 ± 7.5
Liver total cholesterol (mg/g)	2.8 ± 0.14	2.2 ± 0.03^{c}
Liver 25-HC (ng/g)	20.0 ± 1.4	14.9 ± 1.3^{c}

Different groups of animals were used for measurements of plasma lathosterol, plasma cholesterol, liver cholesterol and liver 25-HC. Data for body and liver weight represent the mean ± S. E. M. of nine mice in each group. Data for cholesterol and 25-HC levels are shown as means ± S. E. M. of three and six mice in each group, respectively. Data for lathosterol levels are expressed as a mean ± S. D. of three independent determinations, using pooled plasma from six mice. $^{a}P < 0.01$, $^{b}P < 0.001$ and $^{c}P < 0.05$ versus WT mice

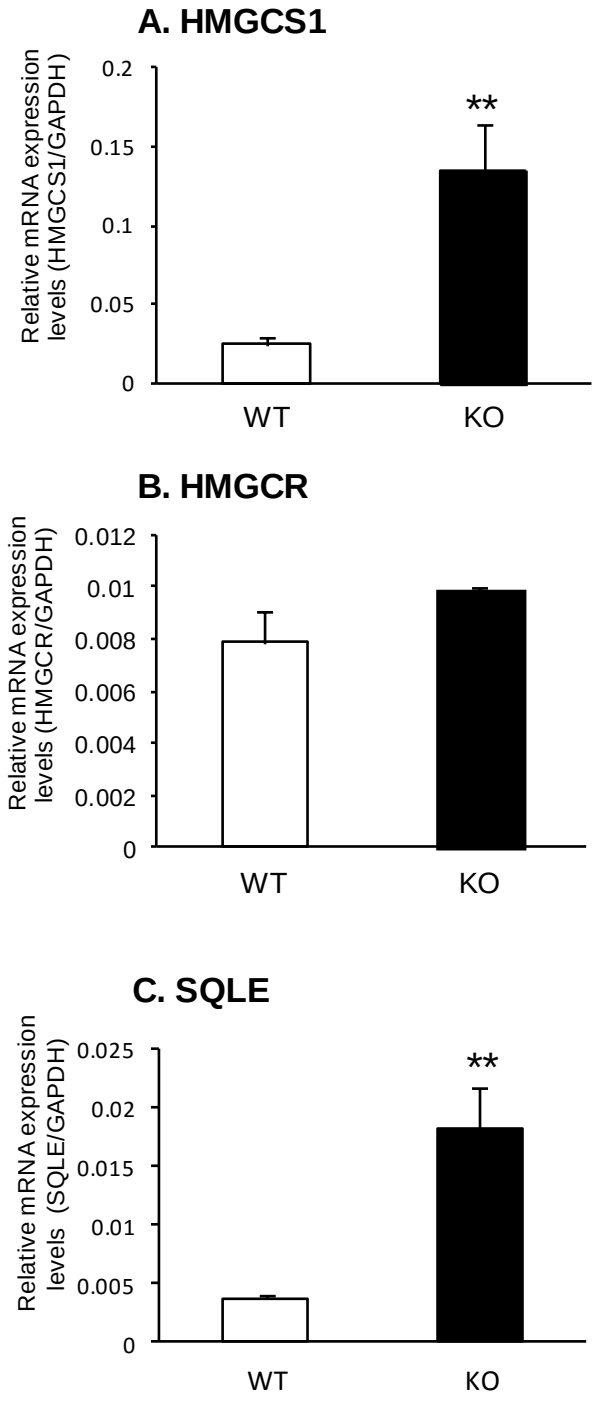

Fig. 2. Expression levels of HMGCS1 (A), HMGCR (B) and SQLE (C) mRNAs in the livers of WT and *Cyp3a*$^{-/-}$ (KO) mice.

Expression levels were normalized by those of GAPDH and are shown as means ± S. E. M. of six mice in each group. cDNAs prepared from each mouse were used for triplicate determination. ***P* < 0.01 versus WT mice.

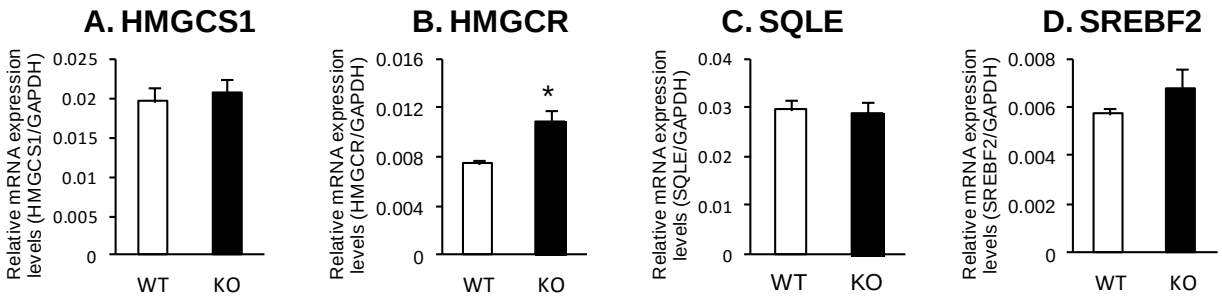

Fig. 3. Expression levels of HMGCS1 (A), HMGCR (B) SQLE (C) and SREBF2 (D) mRNAs in the intestines of WT and *Cyp3a*$^{-/-}$ (KO) mice.

Expression levels were normalized by those of GAPDH and are shown as means ± S. E. M. of six mice in each group. cDNAs prepared from each mouse were used for triplicate determination. *$P < 0.05$ versus WT mice.

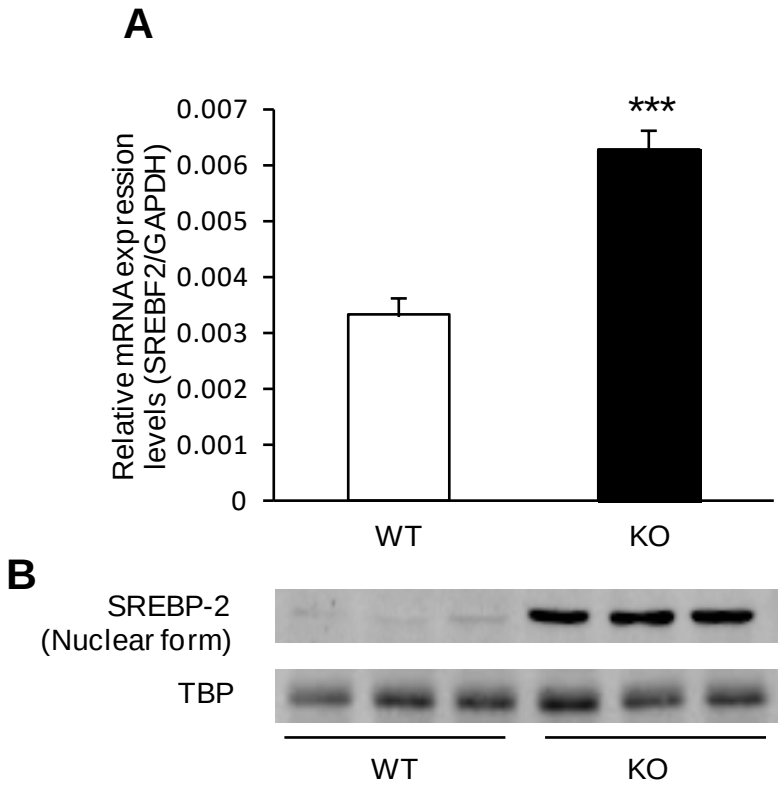

Fig. 4. Expression levels of SREBP2 in the livers of WT and *Cyp3a*$^{-/-}$ (KO) mice.

(A) Expression levels of SREBF2 mRNAs were normalized by those of GAPDH and are shown as means ± S. E. M. of six mice in each group. cDNAs prepared from each mouse were used for triplicate determination. ***$P < 0.001$ versus WT mice. (B) SREBP2 protein was assessed using Western blotting of isolated hepatic nuclear protein. TBP was used as a loading control.

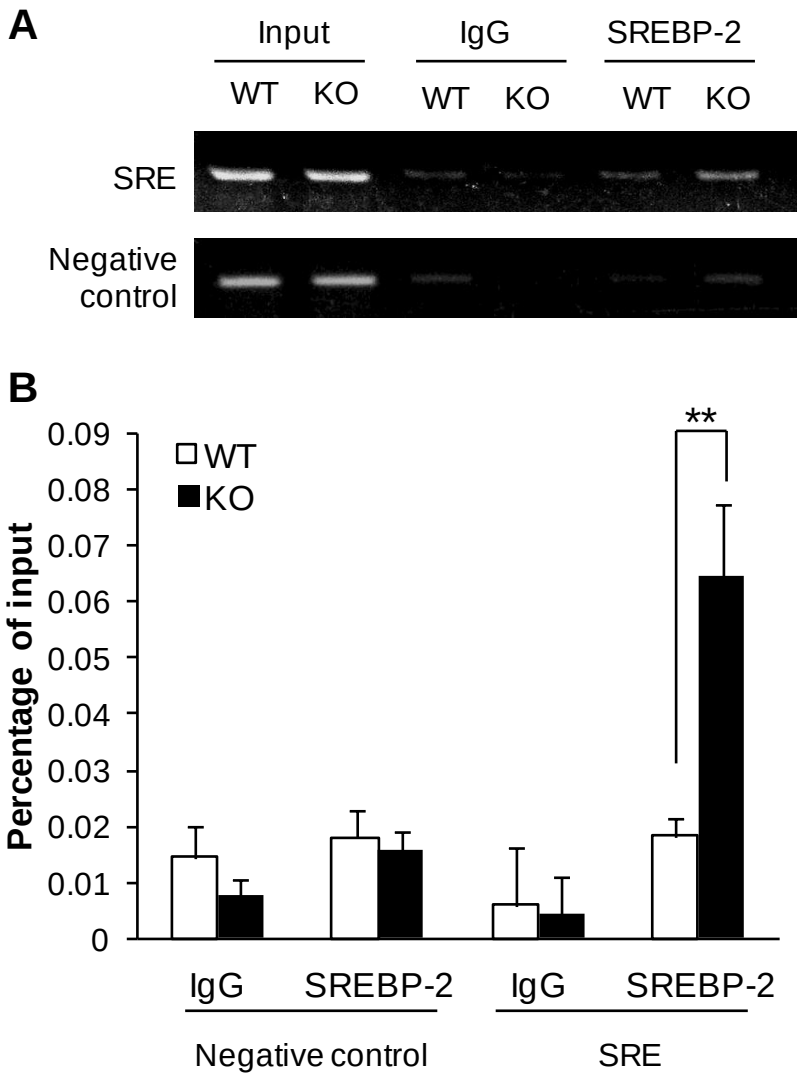

Fig. 5. SREBP2 binding to *Hmgcs1* promoter (-348 to -208) in the livers of WT and *Cyp3a*$^{-/-}$ (KO) mice.

ChIP assay was performed using anti-SREBP2 antibody. Liver tissues from two mice in each group were pooled and subjected to the assay. The immunoprecipitated DNA, along with the DNA isolated before immunoprecipitation (Input), were analyzed by semi-quantitative PCR (A) and quantitative PCR (B). Signals were normalized to input DNA. Data are means ± S.D. of three independent determinations, each performed in duplicate. $^{**}P < 0.01$ versus WT mice.

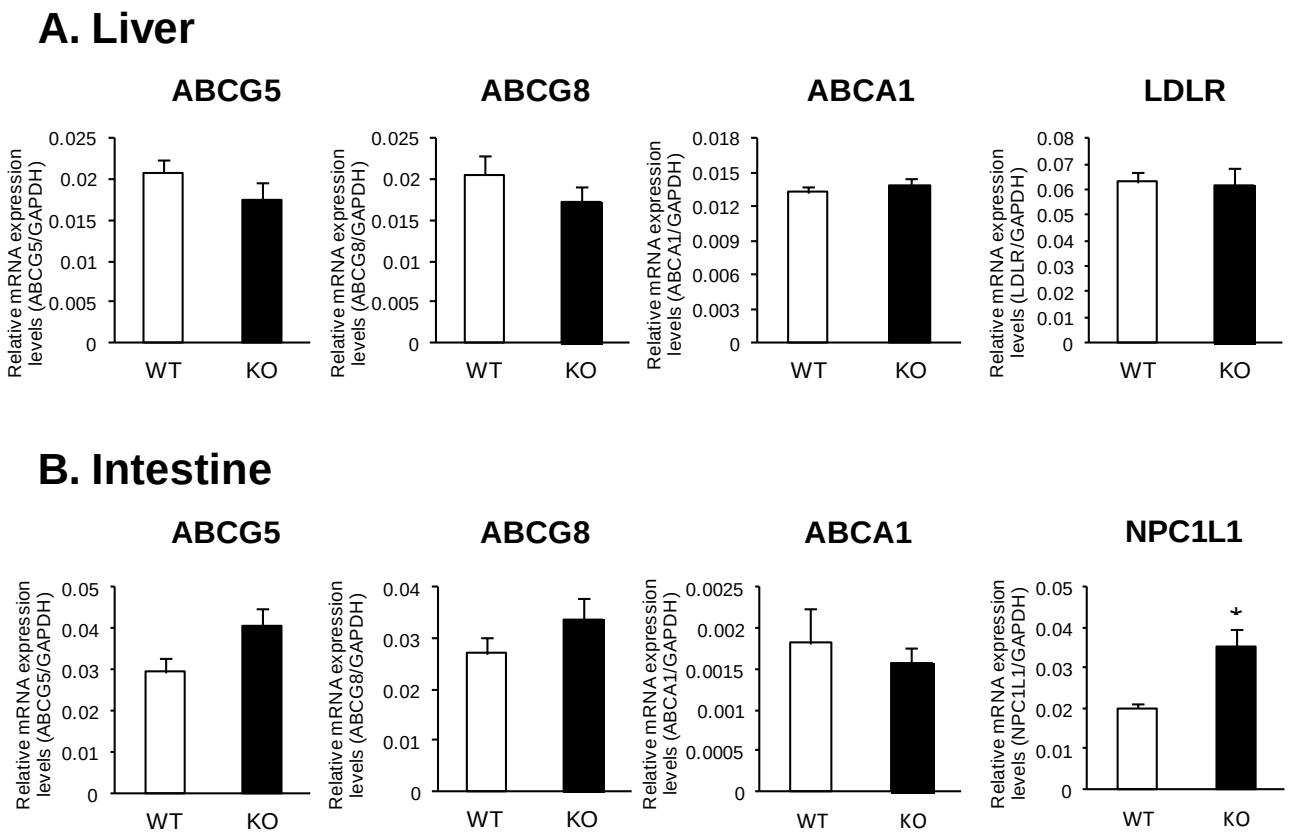

Fig. 6. Expression levels of ABCG5, ABCG8, ABCA1, LDLR and NPC1L1 mRNAs in the livers (A) and intestines (B) of WT and *Cyp3a*$^{-/-}$ (KO) mice.

Expression levels were normalized by those of GAPDH and are shown as means ± S. E. M. of six mice in each group. cDNAs prepared from each mouse were used for triplicate determination. **P* < 0.05 versus WT mice.

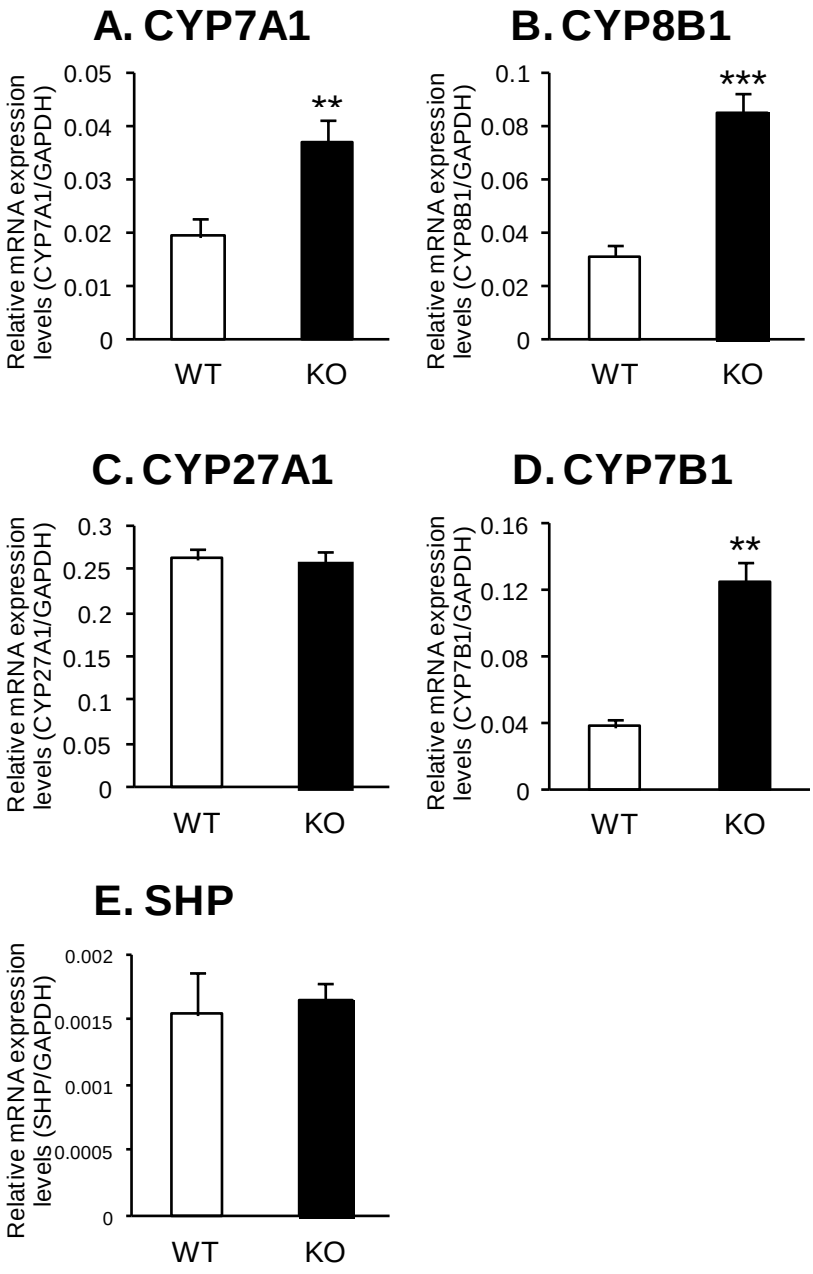

Fig. 7. Expression levels of CYP7A1 (A), CYP8B1 (B), CYP27A1 (C), CYP7B1 (D) and SHP (E) mRNAs in the livers of WT and *Cyp3a*$^{-/-}$ (KO) mice.

Expression levels were normalized by those of GAPDH and are shown as means ± S. E. M. of six mice in each group. cDNAs prepared from each mouse were used for triplicate determination. $^{**}P < 0.01$ and $^{***}P < 0.001$ versus WT mice.

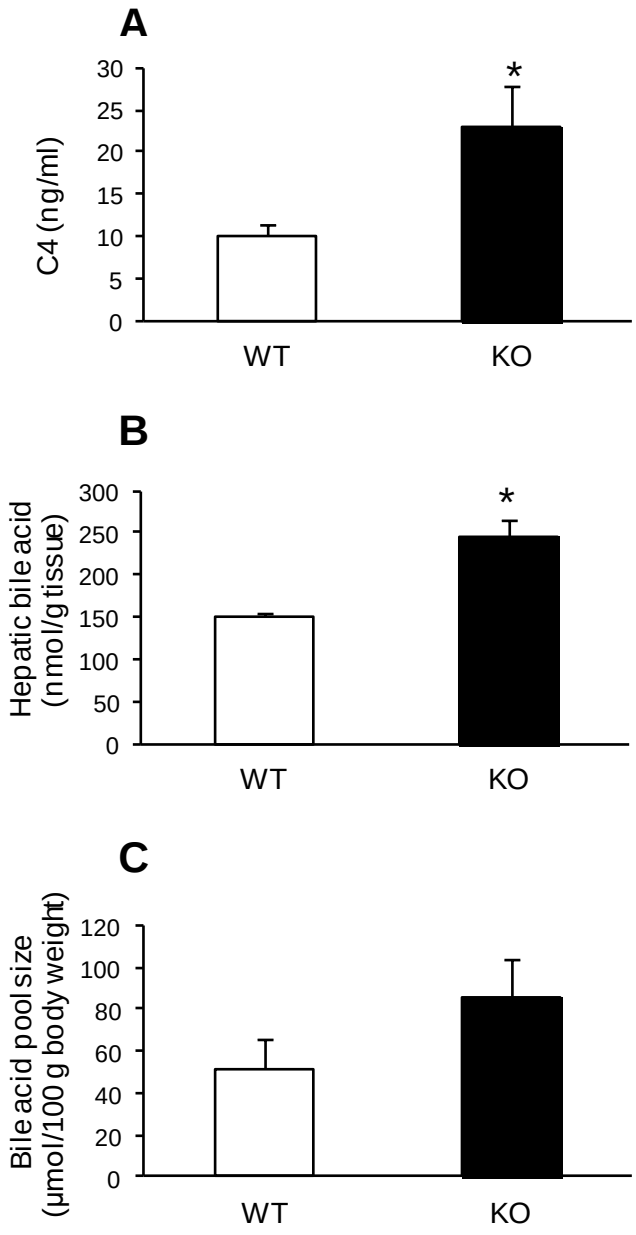

Fig. 8. Concentration of C4 in plasma (A), hepatic bile acid (B) and bile acid pool size (C) of WT and *Cyp3a*$^{-/-}$ (KO) mice.

Plasma C4 concentrations are expressed as a mean ± S. D. of triplicate determinations, using pooled plasma from six mice. Hepatic bile acid levels were expressed as means ± S. E. M. of three mice in each group. Bile acid pool size was determined as total bile acid from liver, gallbladder and intestine. The values of bile acid pool size were shown as means ± S. E. M. of three mice in each group. *$P < 0.05$ versus WT mice.

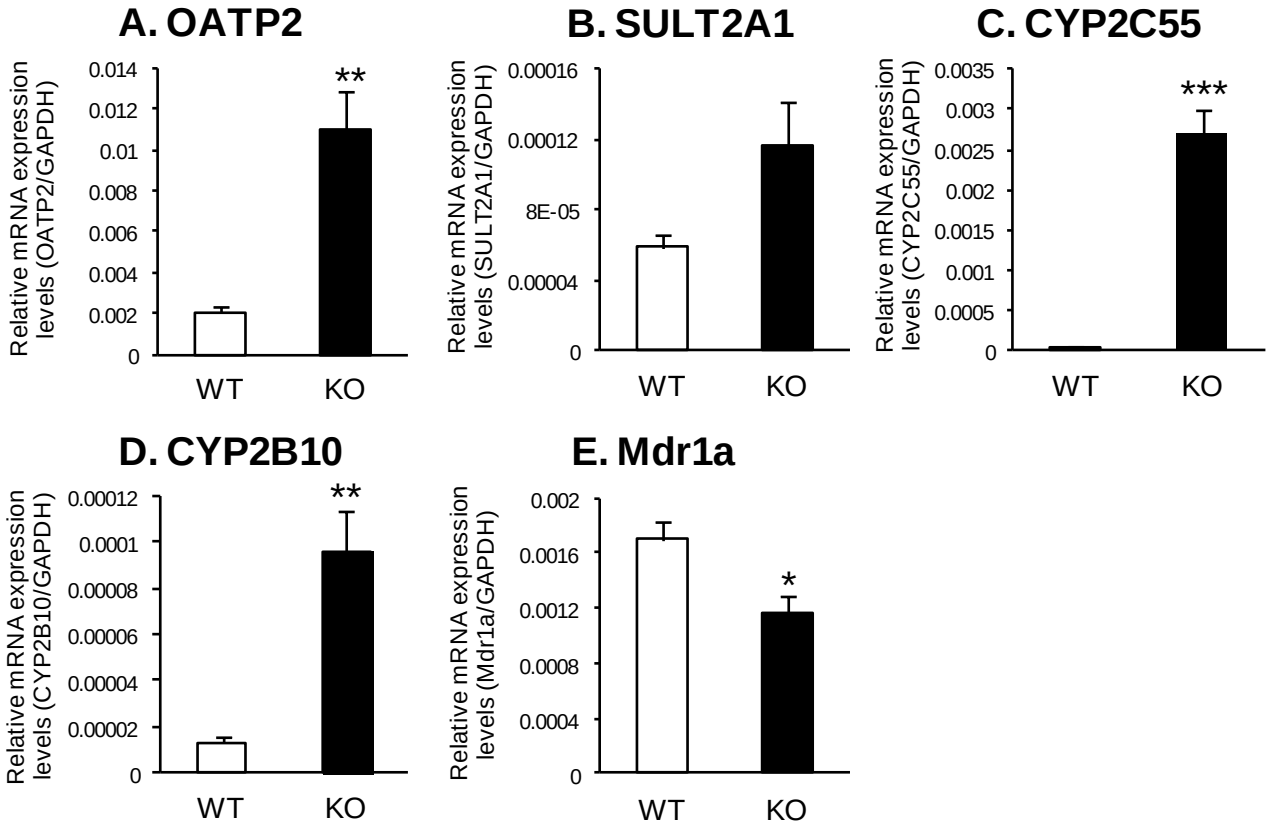

Fig. 9. Expression levels of OATP2 (A), SULT2A1 (B), CYP2C55 (C), CYP2B10 (D) and Mdr1a (E) mRNAs in the livers of WT and *Cyp3a*$^{-/-}$ (KO) mice.

Expression levels were normalized by those of GAPDH and are shown as means ± S. E. M. of six mice in each group. cDNAs prepared from each mouse were used for triplicate determination. *P < 0.05, **P < 0.01 and ***P < 0.001 versus WT mice.

1-4. Discussion

In this study, we showed for the first time that mRNA expression levels of enzymes (*i.e.*, HMGCS1 and SQLE) involved in cholesterol biosynthesis were higher in the livers of *Cyp3a*$^{-/-}$ mice than in the livers of WT mice (Fig. 2). We also found that expression levels of SREBP2, which activates the transcription of these genes [8, 26], were increased in the livers of *Cyp3a*$^{-/-}$ mice compared with those in the livers of WT mice at the levels of mRNA and nuclear protein (Fig. 4). In addition, results of the ChIP assay showed that binding of SREBP2 to the promoter region of the *Hmgcs1* gene was greater in the livers of *Cyp3a*$^{-/-}$ mice than in the livers of WT mice (Fig. 5). These results clearly indicated that SREBP2 was activated in the livers of *Cyp3a*$^{-/-}$ mice, resulting in enhancing transcription of genes encoding enzymes involved in cholesterol biosynthesis. Furthermore, plasma levels of lathosterol in *Cyp3a*$^{-/-}$ mice showed a trend toward higher than those of WT mice, although the difference was not significant (Table 3). Therefore, deficiency of CYP3A enzymes may increase cholesterol synthesis.

Despite the fact that cholesterol biosynthesis was activated in *Cyp3a*$^{-/-}$ mice, total cholesterol levels in the liver were decreased in *Cyp3a*$^{-/-}$ mice compared with those in WT mice (Table 3). Since hepatic cholesterol levels are regulated by influx, efflux and conversion into bile acids of cholesterol, we investigated mRNA expression levels of cholesterol transporters and a rate-limiting enzyme in bile acid biosynthesis in WT and *Cyp3a*$^{-/-}$ mice. Results of the present study showed that deficiency of CYP3A enzymes did not affect mRNA expression levels of ABCG5, ABCG8, ABCA1 and LDLR in the liver (Fig. 6A). In the intestine, mRNA expression levels of ABCG5, ABCG8 and ABCA1 were similar between WT and *Cyp3a*$^{-/-}$ mice, and deficiency of CYP3A enzymes did not decrease mRNA levels of cholesterol influx transporter NPC1L1 (Fig. 6B). On the other hand, mRNA levels of CYP7A1, CYP8B1 and CYP7B1 were significantly higher in *Cyp3a*$^{-/-}$ mice than in WT mice (Fig. 7). Plasma concentration of C4 and total bile acid levels in the liver were also significantly higher in *Cyp3a*$^{-/-}$ mice than in WT mice (Figs. 8A and 8B). Therefore, it is thought that reduction of hepatic total cholesterol in *Cyp3a*$^{-/-}$ mice was due to enhanced bile acid synthesis rather than alteration in cholesterol transport in the intestine and liver. This idea is supported by results of a previous study showing that hepatic total cholesterol in rat CYP7A1 transgenic hamsters maintained on a western-type diet was decreased because of enhancement of bile acid synthesis [45]. Conversely, *CYP7A1* mutation, which leads to loss of active sites and function, resulted in suppression of the classical pathway of bile acid synthesis and substantial cholesterol accumulation in the human liver [46]. These findings suggest that reduction of hepatic total cholesterol in *Cyp3a*$^{-/-}$ mice would be the consequence of enhanced bile acid synthesis by CYP7A1, CYP8B1 and CYP7B1.

In this study, we found that deficiency of CYP3A enzymes enhanced expression of CYP7A1 and CYP8B1 (Figs. 7A and 7B). It is well known that *Cyp7a1* gene is transcriptionally activated by liver X receptor α (LXRα) [47]. However, no difference between WT and *Cyp3a*$^{-/-}$ mice was observed in the expression levels of ABCG5, ABCG8 and ABCA1, which were typical target genes of LXRα

(Fig. 6) [27, 48]. Therefore, it was not suggested that deficiency of CYP3A enzymes was involved in the activation of LXRα. Expression of CYP7A1 and CYP8B1 is regulated by farnesoid X receptor (FXR), which suppresses the transcription of genes through activation of SHP [49, 50]. However, deficiency of CYP3A enzymes did not affect the expression of SHP mRNA (Fig. 7E). Expression of CYP7A1 is also suppressed through activation of PXR [43, 44]. If deficiency of CYP3A enzymes could lead to deactivation of PXR through decreased formation of PXR ligands, expression of CYP7A1 might be increased. However, deficiency of CYP3A enzymes increased the expression of four target genes of PXR except for Mdr1 (Fig. 9). Therefore, it is hard to consider that PXR were deactivated in the livers of *Cyp3a*$^{-/-}$ mice compared with those of WT mice. Taken together with these findings, enhanced expression of CYP7A1 and CYP8B1 in *Cyp3a*$^{-/-}$ mice may be regulated by factors except for LXRα, FXR and PXR. Further studies are needed to clarify the mechanism.

Several studies have shown that CYP3A enzymes are involved in cholesterol metabolism. It has been reported that CYP3A enzymes catalyze 4βHC and 25HC of cholesterol [5, 6]. 4β-HC was recently shown as an LXR activator [51], whereas its role in the cholesterol synthesis is unclear. On the other hand, 25HC is well known as a negative regulator in the cholesterol synthesis [35]. 25HC and other oxysterols suppress cholesterol biosynthesis by suppressing proteolytic activation of SREBP2 [35]. Although production of 25-HC is also produced by microsomal cholesterol 25-hydroxylase [10], mitochondrial CYP27A1 [11, 12] and non-enzymatic autoxidation of cholesterol [13], results of the present study showed that levels of 25-HC in the livers of *Cyp3a*$^{-/-}$ mice were significantly lower than those in WT mice (Table 3). Therefore, it is suggested that deficiency of CYP3A lead to reduction of 25HC synthesis, resulting in activation of SREBP2.

25HC is metabolized to 7α, 25-diHC by CYP7A1 and CYP7B1 [52]. Results of the present study showed that the expression of CYP7A1 and CYP7B1 in the livers of *Cyp3a*$^{-/-}$ mice were higher than those of WT mice (Fig. 7). Therefore, up-regulation of these genes may also relate to the reduction of 25HC and the activation of SREBP2 in the livers of *Cyp3a*$^{-/-}$ mice. In addition, it is possible that deficiency of CYP3A enzymes enhanced bile acid synthesis with consumption of cholesterol in the liver, resulting in compensatory up-regulation of cholesterol synthesis.

Interestingly, it has been reported that mice fed a 25-HC containing diet (0.25%) show decreased body weight relative to control mice fed the basal diet [53]. In this study, deficiency of CYP3A enzymes caused increase of body and liver weight (Table. 3). Taken together, decreased oxysterols appear to increase body and liver weight of *Cyp3a*$^{-/-}$ mice, although the mechanism is unclear.

Activated SREBP2 up-regulates the expression of numbers of genes involved in cholesterol synthesis and uptake. However, there are large differences in the effects of SREBP2 on the expression of mRNA [54]. Therefore, no change of the expression of LDLR mRNA in the livers of *Cyp3a*$^{-/-}$ mice may be due to the small response to SREBP2 activation.

The results of the present study showed that SREBP2 is activated in the livers of *Cyp3a*$^{-/-}$ mice possibly due to reduction of the formation of 25-hydrxy-cholesterol and/or other cholesterol

metabolites, which may result in enhancement of the transcription of genes encoding enzymes involved in cholesterol biosynthesis. Interestingly, it has been reported that feeding a low-cholesterol diet to mice attenuates hepatic CYP3A11 expression by activating hepatic SREBP2 [55]. Activated SREBP2 has been suggested to interact with peroxisome proliferator-activated receptor γ coactivator-1α (PGC-1α) in the mouse liver, resulting in reduced PGC-1α recruitment to hepatocyte nuclear factor-4α on the CYP3A11 promoter and subsequent down-regulation of CYP3A11 expression [55]. Conversely, feeding high-cholesterol diets to rats has been reported to increase expression and activity of CYP3A [56]. Similarly, a cholesterol and cholic acid-supplemented diet increased mRNA expression levels of mouse CYP3A11 [57]. These findings are considered to be important, being coupled with the findings in the present study that transcription of genes encoding enzymes responsible for the synthesis of cholesterol was enhanced by activation of SREBP2 in *Cyp3a*$^{-/-}$ mice. We are tempted to speculate that in the environment of a low-cholesterol diet, CYP3A enzymes are down-regulated, and down-regulated CYP3A enzymes attenuate the formation of oxysterols such as 25-HC. This reduction of oxysterols would activate SREBP2 and enhance expression of genes encoding enzymes involved in cholesterol biosynthesis, which may increase hepatic cholesterol biosynthesis to restore cholesterol levels. In the environment of a high-cholesterol diet, a reverse phenomenon may occur. Thus, CYP3A enzymes may play an important role in maintaining a constant level of hepatic cholesterol, irrespective of environmental changes in dietary cholesterol. However, this is only a hypothesis. Further studies are needed to clarify the role of CYP3A enzymes in the homeostasis of cholesterol in the liver.

In summary, the results of the present study showed that expression of genes encoding enzymes involved in cholesterol biosynthesis is enhanced *via* the activation of SREBP2 in the livers of *Cyp3a*$^{-/-}$ mice, possibly due to the decreased formation of oxysterols. Since dietary cholesterol has been reported to affect gene expression of CYP3A enzymes [55-57], the present observations suggest that CYP3A enzymes play a role in maintaining cholesterol levels at a constant level in the liver. The results of the present study also showed that total cholesterol levels were also decreased by 20% in the livers of *Cyp3a*$^{-/-}$ mice, possibly due to enhanced bile acid synthesis by elevation of CYP7A1 in *Cyp3a*$^{-/-}$ mice. Further studies are required to clarify the role of CYP3A enzymes in the homeostasis of cholesterol in the liver.

Chapter Ⅱ

Studies on the effects of *Cyp3a* deficiency on AR activity and cholesterol synthesis in prostate

2-1. Introduction

Androgens play critical roles in several stages of development and maintenance of the prostate through activation of AR. Testosterone is a principal androgen that circulates in the bloodstream largely bound to sex hormone–binding globulin (SHBG) and diffuses into a target organ as a free form of testosterone [58]. In the prostate, testosterone is converted by steroid 5α-reductase 2 (SRD5A2) into dihydrotestosterone (DHT), having higher affinity than testosterone to the AR, and activates the AR. The activated AR translocates from the cytoplasm to the nucleus, dimerizes, binds to the androgen response element (ARE) in the genome sequences of target genes, and regulates their transcription.

Testosterone is inactivated through hydroxylation and conjugation pathways [59, 60]. 6β-Hydroxylation is the main pathway among testosterone hydroxylation processes in the liver microsome. Testosterone 6β-hydroxylation is mainly catalyzed by CYP3A [7, 61], which is expressed in the liver predominantly and is also expressed in other organs including the prostate [62-65]. Recently, Zhang *et al*. [18] reported that treatment with pregnenolone 16α-carbonitrile, an inducer of CYP3A, reduces either the plasma testosterone levels or prostate weights in castrated mice. This finding suggests that CYP3A is one of the regulators for circulating testosterone and its effects on the prostate [14]. However, it remains unclear whether a decreased state of CYP3A activity affects the systemic level of testosterone and its effects on the prostate.

Androgens enhance cholesterol synthesis in the LNCaP line of cells, an androgen-dependent prostate cancer cell line, by the following mechanism: androgens stimulate the processing of SREBP2 through AR-mediated activation of SCAP gene transcription [11, 12], and activated SREBP2 increases expression levels of genes involved in the synthesis and transport of cholesterol such as *Hmgcs1*, *Hmgcr*, and *Ldlr* [8]. However, whether androgens stimulate these processes in the *in vivo* prostate remains unclear.

The purpose of the present study was to clarify whether a reduced state of CYP3A activity affects the systemic levels of testosterone and its effect on the prostate. To accomplish this purpose, we studied the effects of *Cyp3a* deficiency on circulating testosterone levels and prostatic expression levels of genes regulated by the AR using *Cyp3a*-knockout (*Cyp3a*$^{-/-}$) mice. We also studied the expression levels of genes involved in cholesterol synthesis and total cholesterol content in the prostate of *Cyp3a*$^{-/-}$ mice in order to explore the possibility that activation of the AR affects cholesterol synthesis *via* the SCAP-SREBP2 pathway in the prostate.

2-2. Materials and Methods

2-2-1. Chemicals

Testosterone and formaldehyde were purchased from Wako. 6βHT was purchased from Sigma-Aldrich. Bicalutamide was purchased from Tokyo Chemical Industry (Tokyo, Japan). High-performance liquid chromatography (HPLC) grade acetonitrile, chloroform and methanol purchased from Wako were also used in our experiments.

2-2-2. Animals

We previously reported the generation of *Cyp3a*$^{-/-}$ mice that lacked six *Cyp3a* isoforms (*Cyp3a13/57/44/11/25/59*) [33]. Briefly, conventional gene targeting and Cre-loxP-mediated chromosomal deletion were, respectively, used to generate *Cyp3a13*$^{-/-}$ and *Cyp3a57-59*$^{-/-}$ lines, after which the two lines were mated to generate *Cyp3a*$^{-/-}$ mice. The size between the *Cyp3a57-59* gene cluster and a *Cyp3a13* gene is ~5 Mb, and several genes are located between the loci, so the two knockout lines were generated independently. The generated *Cyp3a*$^{-/-}$ mice were backcrossed to C57BL/6JJcl mice (CLEA) more than five-generation. The deficiency of mRNA expression of the six *Cyp3a* isoforms in the livers and prostates of *Cyp3a*$^{-/-}$ mice was then confirmed [33] (Fig. 10). In these studies, C57BL/6JJcl mice were used as WT mice.

All experiments were performed using male mice between 10 and 11 weeks of age, and all experimental animals were kept in a temperature-controlled environment with a 12-hr light/dark cycle. The light-cycle hours were between 7 AM and 7 PM. The mice weighting 23.3 ± 0.18 g for WT mice and 23.5 ± 0.43 g for *Cyp3a*$^{-/-}$ mice received a chow diet containing 0.1% cholesterol (CE-2, CLEA). The mice were sacrificed between 10 and 11 AM without a prior fast. The plasma, livers, and total prostates (including the anterior, ventral, lateral, and dorsal prostate lobes) were collected immediately and stored at -80ºC until usage. The present study was conducted in accordance with the Guidelines for the Care and Use of Laboratory Animals, as adopted by the Committee on Animal Research of Tottori University and Chiba University.

2-2-3. Treatment with bicalutamide

Male *Cyp3a*$^{-/-}$ mice were 10 weeks of age at the time of drug administration. Bicalutamide was formulated in polyethylene glycol 400 (PEG400)/Tween 80 (80:20 by volume) and administered orally by gavage once per day in 10 mg/kg for 7 days. A control group was administered the vehicle daily. Prostate samples were frozen at -80℃ until analysis.

2-2-4. RNA isolation and cDNA synthesis

Total RNA was isolated from prostate and liver tissues, extracted using ISOGEN (Nippon Gene), and then purified using RNeasy columns (Qiagen) in accordance with the manufacturer's instructions. All specimens were then treated with RNase-free DNase I (Wako). The cDNA was generated with a random hexamer using a High-Capacity cDNA Reverse Transcription Kit (Applied Biosystems).

2-2-5. Analysis of mRNA levels

Expression levels of *Cyp3a11/13/16/25/57/59* were determined by semi-quantitative polymerase chain reaction (PCR) analysis as described previously [66]. The primer sequences used to amplify *Cyp3a11/13/16/25/57/59*, *Hmgcs1*, *Hmgcr, Ldlr and Srebf2* have been described previously [33, 66]. Specific primers for *D-dopachrome tautomerase (Ddt), protein kinase C delta (Prkcd), spermine-binding protein (Sbp)* and *Scap* are listed in Table 4. Expression levels were measured by SYBR Green-based real-time PCR using KAPA SYBR Fast ABI Prism 1000 (KAPA Biosystems, Woburn, MA) carried out on an EcoReal-time PCR system (Illumina). The mRNA expression levels were normalized using 18S rRNA as an endogenous control gene.

2-2-6. Preparation of liver microsomes

Liver tissues were homogenized in ice-cold 1.15% KCl and microsomes were isolated by differential centrifugation. Briefly, liver homogenate was centrifuged at 9000 × g for 20 min at 4ºC. The resultant supernatant was then ultra-centrifuged at 105,000 × g for 1 h at 4ºC. The microsomal pellet was then washed and resuspended in 100 mM sodium phosphate buffer (pH 7.4) and stored at −80ºC until analysis. Protein concentrations were determined using a DC protein assay kit (Bio-Rad) according to manufacturer's instructions.

2-2-7. Enzyme assay

Testosterone 6β-hydroxylase activity was determined as described previously with some modifications [67]. Briefly, the basic incubation mixture contained 0.05 mg/ml liver microsomes, 0.1 mM EDTA, 100 mM potassium phosphate buffer (pH 7.4), an NADPH-generating system (0.5 mM $NADP^+$, 2 mM glucose-6-phosphate, 1 IU/ml glucose-6-phosphate dehydrogenase, 4 mM $MgCl_2$) and a substrate (30 μM testosterone), in a final volume of 250 μl. The mixtures were preincubated for 1 min at 37ºC, and reactions were initiated by the addition of 25 μl of the NADPH-generating system. After 45 min, incubation was stopped by the addition of 100 μl of acetonitrile, followed by the addition of 50 μl of 1 μg/ml diazepam in methanol as an internal standard. Next, the incubated solution was mixed with 500 μl of acetonitrile and 300 μl of 3 M NaCl and then centrifuged at 1000 × g for 15 min,

after which 400 μl of the supernatant (organic layer) was transferred to a new tube and dried under vacuum conditions. The residue was reconstituted with 300 μl of a mobile phase consisting of 10 mM potassium phosphate buffer (pH 7.4) and methanol (2/3, v/v) with a flow rate of 0.9 ml/min. In the next step, an aliquot containing 100 μl of the reconstituted sample was subjected to HPLC analysis using a Hitachi L-7000 model HPLC system (Tokyo, Japan) consisting of an L-7400 UV detector and a CAPCELL PAK C18 UG120 column (4.6 mm × 250 mm, 5 mm; Shiseido, Tokyo, Japan). The eluent was monitored at a wavelength of 245 nm.

2-2-8. Preparation of whole cell lysate

Pooled prostate tissues (20 mg) from six mice were homogenized by mashing with a micro homogenizer pastle in 100 μl of lysis buffer [20 mM Hepes, 420 mM NaCl, 1.5 mM $MgCl_2$, 0.2 mM EDTA and 1% (v/v) NP40 supplemented with 1 mM PMSF and 0.1% (v/v) proteinase inhibitor cocktail (Merck Millipore, Billerica, MA)], incubated for 30 min at 4ºC, and then centrifuged at 14000 × g for 5 min at 4ºC. The supernatants were then transferred to new tubes and stored at −80ºC until used. Protein concentrations were determined using a DC protein assay kit (Bio-Rad) according to the manufacturer's instructions.

2-2-9. Western blot analysis

Whole cell lysates (20 μg/lane) were separated by SDS-polyacrylamide gel electrophoresis and transferred to a nitrocellulose membrane. After 1-hr incubation with blocking buffer (0.05% Tween 20 in phosphate buffered saline (PBS) containing 5% skim milk), the membrane was probed for 1 hr at room temperature using an anti-SCAP goat antibody (1:200 dilution, sc-9675, Santa Cruz Biotechnology) and an anti-SREBP2 rabbit antibody (1:200 dilution, ab30682, Abcam). An anti-β-actin mouse antibody (1:5,000 dilution, Sigma-Aldrich) and an anti-GAPDH rabbit antibody (1:2,000 dilution, Sigma-Aldrich) were used as an internal control. After washing, the membrane was incubated with a peroxidase-conjugated secondary antibody for 1 hr at room temperature. The secondary antibodies used were an anti-rabbit IgG (1:50,000 dilution, Sigma-Aldrich), an anti-mouse IgG (1:50,000 dilution, Abcam) and an anti-goat IgG (1:20,000 dilution, Sigma-Aldrich). The anti-SCAP, anti-β-actin and anti-GAPDH antibodies were diluted with 0.05% Tween 20 in PBS containing 3% bovine serum albumin (BSA). The anti-SREBP2 antibody was diluted with Can Get Signal Solution 1 (TOYOBO, Osaka, Japan). Protein bands were visualized *via* ECL Western Blotting Detection Reagents (GE Healthcare) and ImmunoStar LD (Wako) using LAS-4000 (GE healthcare) and quantified by ImageQuant TL (ver. 8.1, GE Healthcare).

2-2-10. ChIP assay

A ChIP assay was conducted as described previously [66]. In brief, pooled prostate tissues (60 mg) from six mice were minced and fixed by 1% formaldehyde, after which the extracted nuclei were immunoprecipitated with polyclonal anti-AR rabbit antibody (sc-816, Santa Cruz) or rabbit IgG-ChIP grade (ab37415, Abcam). DNA samples were measured by real-time PCR using SYBR Green-based real-time PCR with KAPA SYBR Fast ABI Prism 1000 (KAPA Biosystems). PCR was carried out with primers encompassing the region containing the ARE site (-539 bp to -438 bp in *Sbp* promoter and -209 bp to -102 bp in *Prkcd* promoter) and the non-specific region (+11,862 bp to +11,948 bp in *Sbp* gene) as a negative control. The PCR conditions for *Sbp* promoter were one cycle of pre-denaturation at 95°C for 10 min, 45 cycles of denaturation at 95°C for 15 sec, annealing at 58°C for 30 sec, and elongation at 72°C for 15 sec. The PCR conditions for *Prkcd* promoter were one cycle of pre-denaturation at 95°C for 10 min, 45 cycles of denaturation at 95°C for 15 sec, annealing and elongation at 60°C for 30 sec. The primers used are as follows: *Sbp*/ARE, 5'-CCCAGTATAGCATCATCATCAACA-3' and 5'-AAATGCTGGAACTACCTGTGAATC-3': *Prkcd*/ARE, 5'-GCCAGCAGGAAGAGGAATGA-3' and 5'-GGCTTCCCCAACTACTTGCG-3': *Sbp*/negative control, 5'-GGACACTTCTGGAGCCTGAACT-3' and 5'-AGCTGGAAGCTGGAGAGAAATC-3'.

2-2-11. Analysis of testosterone and DHT levels

Hepatic total testosterone levels were determined by HPLC. Pooled liver tissue (600 mg) from six mice was homogenized in 1 ml of PBS (-) and mixed with 10 μl of 1 μg/ml diazepam as an internal standard. Next, the homogenates were extracted with 20 μl of 2 M sodium hydroxide and 5 ml of chloroform. The mixture was vigorously mixed for 1 min and then centrifuged at 2000 × g for 15 min. The organic layer was then transferred to a new tube and dried under vacuum conditions. The residue was resolved with 200 μl of mobile phase. One hundred μl of the reconstituted sample was analyzed by an HPLC system as described in the enzyme assay section, except that the mobile phase consisted of 10 mM potassium phosphate buffer (pH 7.4) and methanol (37/63, v/v).

Total plasma and prostatic testosterone levels and free plasma testosterone levels were measured using a Free Testosterone ELISA Kit (Cusabio Biotech, Hubei, China). To analyze total testosterone levels, 10 μl of pooled plasma and 15 mg of pooled prostates from six mice was extracted as described above. The organic layer was dried under vacuum conditions and resolved with 2.5 μl of ethanol and sterilized water 400 μl for plasma or 180 μl for prostates. Free testosterone levels in plasma were then measured without extraction. Next, 50 μl of extracts from plasma and prostates, and 50 d prosnon-extracted plasma were used for total plasma and prostatic testosterone, and free plasma testosterone determination, respectively, according to the manufacturer's instructions. DHT levels in the prostates were measured using a DHT ELISA kit (Cusabio Biotech). Pooled prostates were extracted as described for the testosterone and 50 μl of the extracts were used for determination of DHT levels, according to the manufacturer's instructions. The manufacturer's specifications state that these ELISA assays are highly specific and that there is no significant cross-reactivity or interference

with their analogues.

2-2-12. Analysis of cholesterol levels

The concentration of total cholesterol in the prostate was determined using a Cholesterol E-Test Wako kit (Wako) according to the manufacturer's instructions. Pooled prostate tissue from each of the six mice was used. Prostatic lipids were extracted according to the procedure described in our previous report [66] and then reconstituted in 4% methanol.

2-2-13. Statistical analysis

The number of mice in each group is shown in the legends of figures. Data are shown as means ± S. E. M. or S. D. as described in each figure legend. Statistical analyses were performed by using Statcel (OMS, Saitama, Japan). Comparisons were made with Student's t-test or Welche's t-test. $P < 0.05$ was considered statistically significant.

Table 4. Oligonucleotide primers used in real-time PCR

Name	Direction	Sequence (5' to 3')
DDT	Forward	ACAGCCACCATCCTGGACAA
	Reverse	CCAGAAGGTGAGCACAAGGC
PRKCD	Forward	GATGAAGGAGGCACTCAGCA
	Reverse	CGCATCAGCACAATCTGGAT
SBP	Forward	GTGTTTTCAAGTTCATCAAGGGC
	Reverse	GGGTTCCATAGACATCAGTCCA
SCAP	Forward	CTGCGCATCCTATCCAATTC
	Reverse	AGAATTCCACAGGTCCCGTT

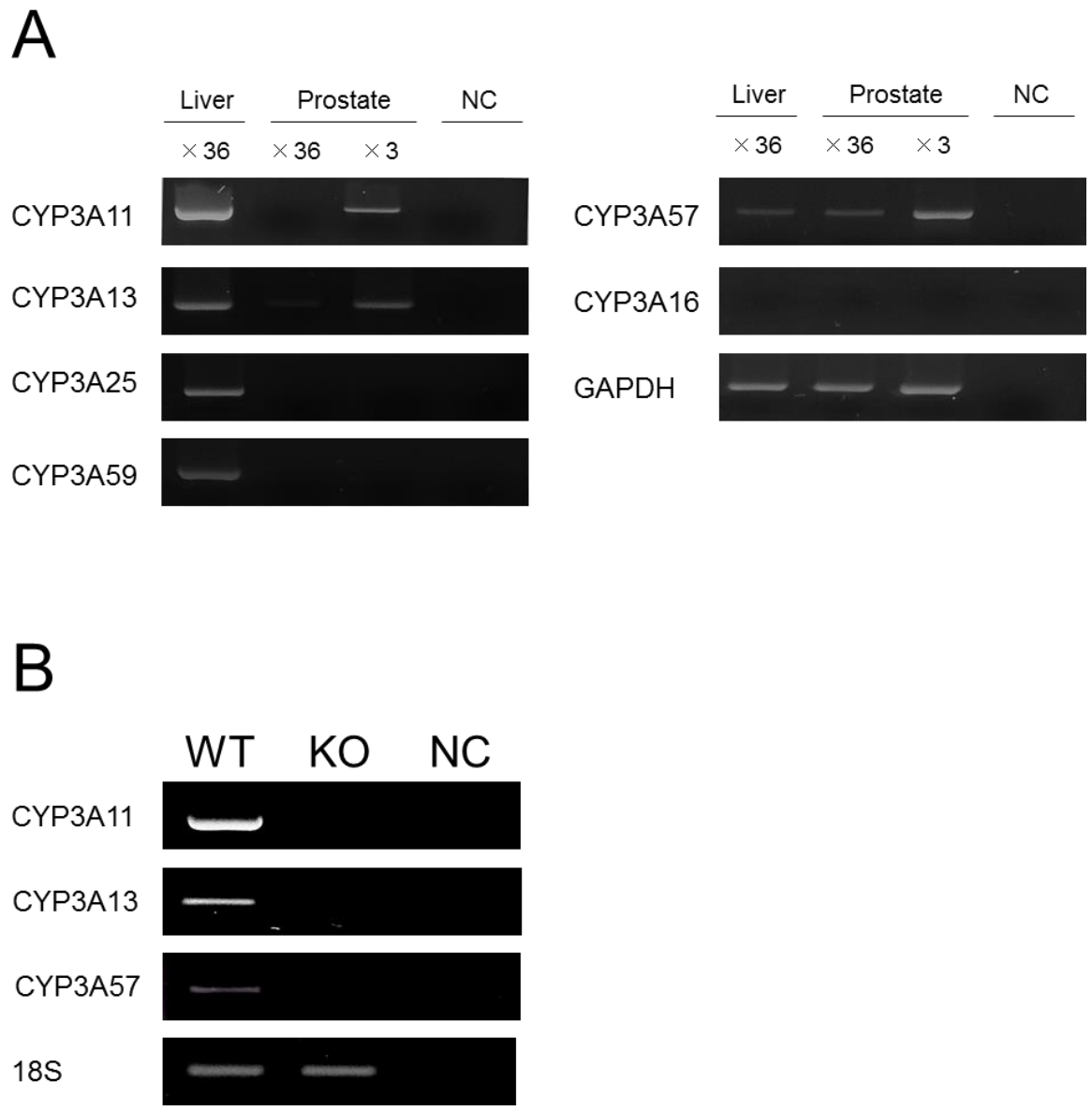

Fig. 10. Expression of *Cyp3a* isoforms in prostates.

A) Expression levels of mouse *Cyp3a* isoforms in livers and prostates of WT mice (n = 6) were analyzed by semi-quantitative RT-PCR. Total RNA (1 μg) extracted from each mouse was subjected to reverse transcription. The aliquots of cDNA products were pooled and diluted for amplification (36 times for liver, 36 and 3 times for prostate). B) Expression levels of mouse *Cyp3a* isoforms in prostates of WT and *Cyp3a*$^{-/-}$ (KO) mice (n = 6) were analyzed by semi-quantitative RT-PCR. Pooled prostate cDNA products were diluted 3 times and subjected to the assay. NC, negative control.

2-3. Results

2-3-1. Effects of *Cyp3a* deficiency on testosterone 6β-hydroxylation

6β-Hydroxylation activities for testosterone were measured in the liver microsomes of *Cyp3a*$^{-/-}$ and WT mice. As shown in Fig. 11, the activity of *Cyp3a*$^{-/-}$ mice was 75% lower than that of WT mice (0.25 *vs*. 1.00 nmol/mg protein/min), whereas activities of testosterone hydroxylation at the other positions showed no significant difference between WT and *Cyp3a*$^{-/-}$ mice (data not shown). We also measured the activities in prostate microsomes of *Cyp3a*$^{-/-}$ and WT mice. However, activities were undetectable in prostate microsomes of *Cyp3a*$^{-/-}$ and WT mice (lower than detection limit, 0.067 nmol/mg protein/min).

2-3-2. Effects of *Cyp3a* deficiency on testosterone levels

Total testosterone levels in the plasma and liver of *Cyp3a*$^{-/-}$ and WT mice were examined. As shown in Figs. 12A and 12B, the levels in the livers and plasma of *Cyp3a*$^{-/-}$ mice were 1.8-fold higher than those in the plasma and liver of WT mice (1.50 *vs*. 0.81 ng/g tissue and 590 vs. 334 pg/ml, respectively). Furthermore, free testosterone levels in the plasma of *Cyp3a*$^{-/-}$ mice were 9.0-fold higher than that in WT mice (218 *vs*. 24.3 pg/ml, Fig. 12B), although there was no significant difference between them in plasma levels of luteinizing hormone, which is a suppressor of testosterone synthesis (data not shown). As shown in Fig. 12C and 12D, total testosterone and DHT levels in the prostates were also 3.3-fold and 1.8-fold higher in *Cyp3a*$^{-/-}$ mice than that in WT mice, respectively (1.66 *vs*. 0.51 ng/g tissue, and 0.72 *vs*. 0.39 ng/g tissue, respectively). In addition, mRNA expression levels of SRD5A2 were also higher in the prostates of *Cyp3a*$^{-/-}$ mice (Fig. 12E). Noting, *Cyp3a*$^{-/-}$ and WT mice used in this study showed no significant difference in prostate weight (data not shown).

2-3-3. Effect of *Cyp3a* deficiency on androgen response

Since increased levels of total testosterone in the prostates of *Cyp3a*$^{-/-}$ mice implies activation of androgen response in the prostates of *Cyp3a*$^{-/-}$ mice, we measured the expression levels of AR target genes. As shown in Fig. 13A, mRNA expression levels of *Sbp, Prkcd, Ddt* and *Scap* were significantly higher in the prostates of *Cyp3a*$^{-/-}$ mice than in the prostates of WT mice. In addition, protein expression levels of SCAP were higher in the prostates of *Cyp3a*$^{-/-}$ mice than those of WT mice (Fig. 13B). Moreover, results of the ChIP assays showed that specific binding of the AR to the ARE-containing region of the *Sbp* and *Prkcd* promoter [68, 69] was significantly more abundant in the prostates of *Cyp3a*$^{-/-}$ mice than in the prostates of WT mice ($P < 0.01$, Fig. 13C). The degree of binding of the AR to the non-specific region was low and showed no difference between *Cyp3a*$^{-/-}$ and WT mice.

2-3-4. Effects of *Cyp3a* deficiency on mRNA expression levels of target genes of SREBP2 and cholesterol contents in the prostate

Since mRNA expression levels of *Scap* were elevated in the prostates of *Cyp3a*$^{-/-}$ mice, we determined whether SREBP2 was activated. As shown in Fig. 14A, protein expression levels of mature SREBP2, an active form, were higher in the prostates of *Cyp3a*$^{-/-}$ mice than those of WT mice. Next, we examined expression levels of target genes involved in the synthesis and transport of cholesterol. As shown in Fig. 14B, mRNA expression levels of *Hmgcr*, *Hmgcs1* and *Srebf2* were significantly higher in the prostates of *Cyp3a*$^{-/-}$ mice than in the prostates of WT mice. The expression levels of *Ldlr* were also higher in the prostates of *Cyp3a*$^{-/-}$ mice than in the prostates of WT mice, although the difference was not significant. Finally, total cholesterol levels were higher in the prostates of *Cyp3a*$^{-/-}$ mice than in the prostates of WT mice (Fig. 14C).

2-3-5. Effects of bicalutamide treatment on mRNA expression levels of target genes of AR and SREBP2 in the prostate of *Cyp3a*$^{-/-}$ mice

To confirm the activation of AR and sequential activation of SREBP2 in the prostates of *Cyp3a*$^{-/-}$ mice, we examined whether treatment of bicalutamide, antiandrogen drug [70], reduced the mRNA expression levels of target genes of AR and SREBP2 in the prostates of *Cyp3a*$^{-/-}$ mice. As shown in Fig. 15, mRNA expression levels of target genes of AR and SREBP2 in the prostates were lower in the *Cyp3a*$^{-/-}$ mice treated with bicalutamide than those treated with the vehicle alone. Noting, bicalutamide treatment to WT mice reduced total cholesterol levels in the prostates (0.13 ± 0.02 *vs*. 0.09 ± 0.01 mg/g tissue, $P < 0.05$), but not in the livers.

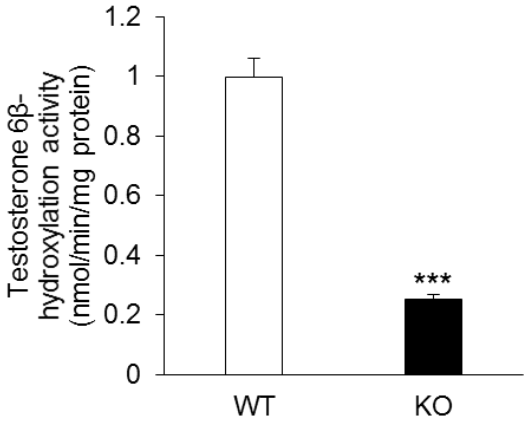

Fig. 11. Testosterone 6β-hydroxylation activities in liver microsomes of WT and *Cyp3a*$^{-/-}$(KO) mice.

Testosterone (30 μM) was incubated with liver microsomes of WT and KO mice. Data are shown as means ± S. E. M (n = 5) of three independent determinations, each performed in duplicate. ***P < 0.001 versus WT mice.

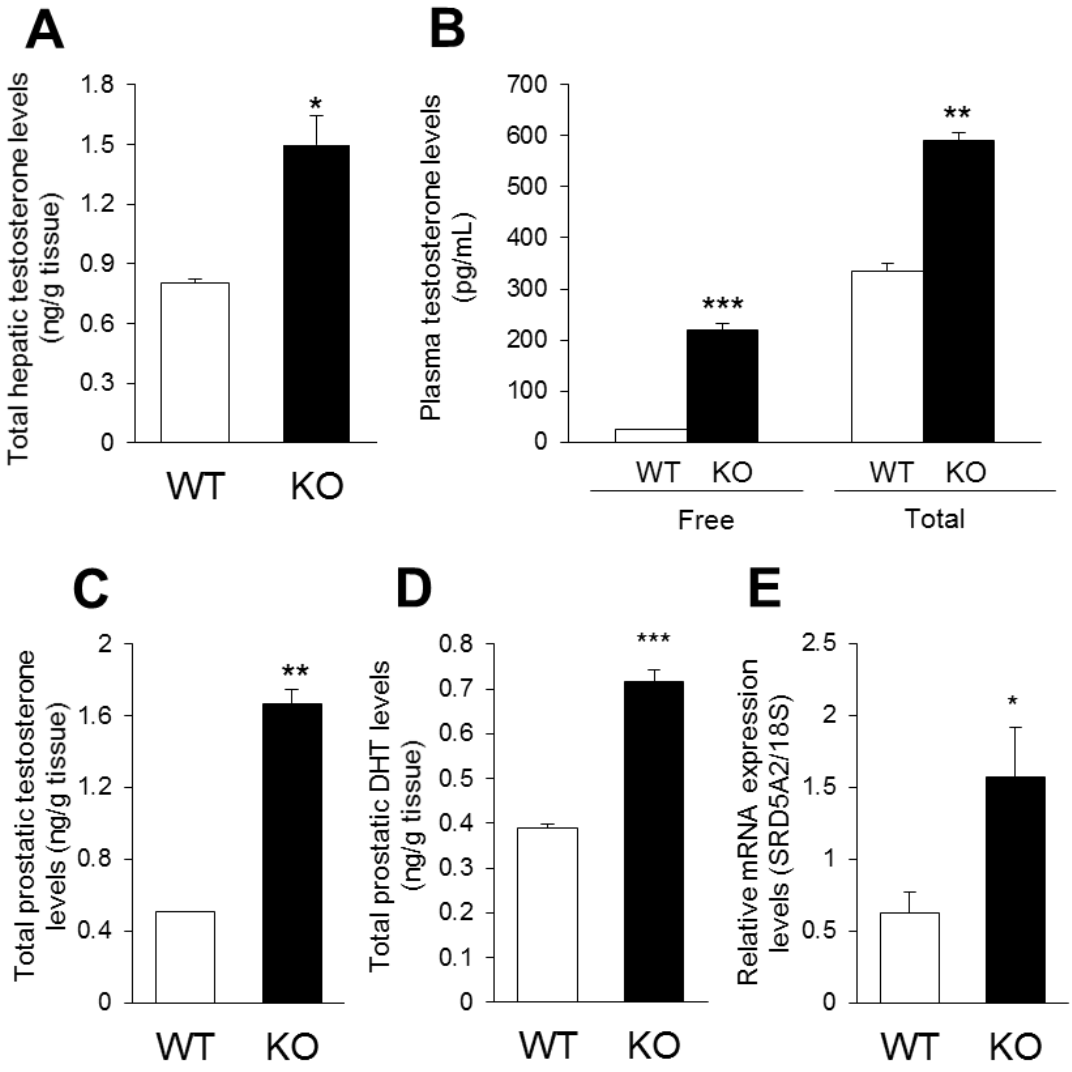

Fig. 12. Androgen levels and mRNA expression levels of *Srd5a2* in WT and *Cyp3a*$^{-/-}$ (KO) mice.
A) Levels of total hepatic testosterone in WT and KO mice were determined by HPLC using pooled liver tissue from six mice. B) Levels of total and free plasma testosterone in WT and KO mice were determined by ELISA using pooled plasma from six mice with or without extraction, respectively. C and D) Levels of total prostatic testosterone and DHT in WT and KO were measured by ELISA using pooled prostates from six mice. Data are shown as means ± S.D. of triplicate determination. E) The mRNA expression of *Srd5a2* were determined and normalized by the expression levels of 18S rRNA. Data are shown as means ± S. E. M. (n = 6) of three independent determinations, each performed in duplicate. *P < 0.05, **P < 0.01, ***P < 0.001 versus WT mice.

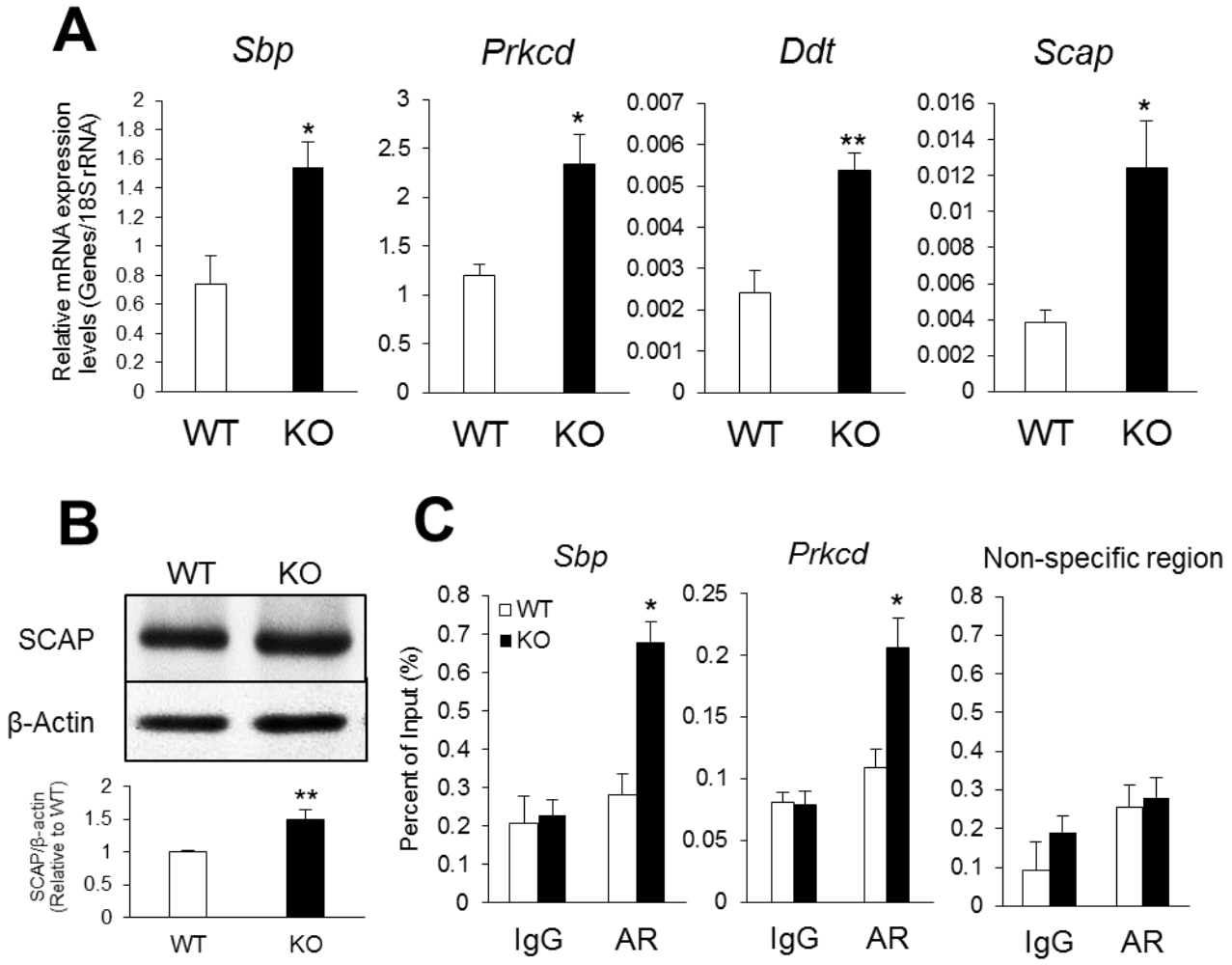

Fig. 13. Expression levels of AR target genes in mRNA (A) and protein (B) and AR binding to *Sbp* and *Prkcd* promoter (C) in the prostates of WT and *Cyp3a*$^{-/-}$ (KO) mice

A) The mRNA expression levels were normalized by expression levels of 18S rRNA. Data are shown as means ± S. E. M. (n = 6) of three independent determinations, each performed in duplicate. B) SCAP protein was assessed by Western blot analysis using pooled lysate of prostates from six mice. β-Actin were used as a loading control. C) ChIP assays were performed using anti-AR antibody. Prostate tissues from five mice in each group were pooled and subjected to the assay. The immunoprecipitated DNA along with the DNA isolated before immunoprecipitation (input) were analyzed by quantitative PCR. Signals were normalized by input DNA. Data are shown as means ± S.D. of triplicate determination. *P < 0.05 and **P < 0.01 versus WT mice.

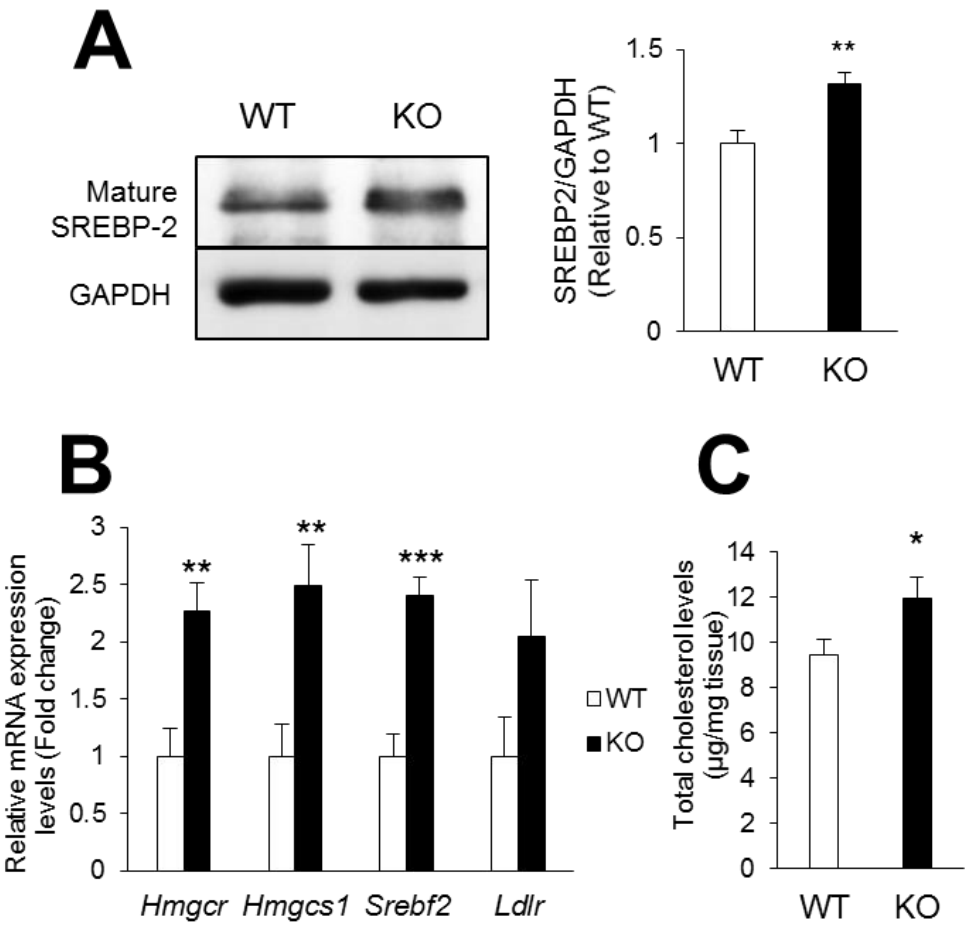

Fig. 14. Protein expression levels of SREBP2 (A), mRNA expression levels of SREBP2 target genes (B) and total cholesterol contents (C) in prostates of WT and *Cyp3a*$^{-/-}$ (KO) mice.

A) Expression levels of mature SREBP2 were studied by Western blot analysis using pooled lysate of prostates from six mice. GAPDH were used as a loading control. B) The mRNA expression levels were normalized by expression levels of 18S rRNA. Data are shown as means ± S. E. M. (n = 6) of three independent determinations, each performed in duplicate. B) Total cholesterol levels in prostates were measured using pooled tissue from five mice. Data for total cholesterol contents in prostates represent the mean ± S. D. of triplicate determination. *P < 0.05, **P < 0.01 and ***P < 0.001 versus WT mice.

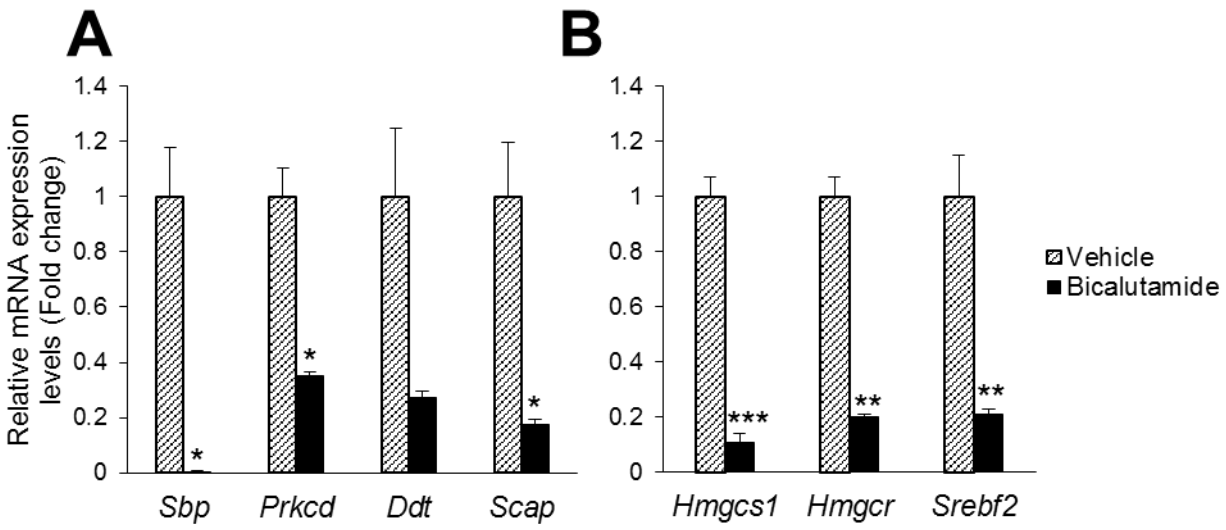

Fig. 15. Effects of bicalutamide treatment on mRNA expression levels of target genes of AR (A) and SREBP2 (B) in the prostates of *Cyp3a*$^{-/-}$ mice.

Cyp3a$^{-/-}$mice were orally treated with bicalutamide (10mg/kg/day, closed bars) or vehicle alone (striped bars) for 7 days. The mRNA expression levels were normalized by expression levels of 18S rRNA. Data are shown as means ± S. E. M. (n = 3) of three independent determinations, each performed in duplicate. *P < 0.05, **P < 0.01 and ***P < 0.001 versus *Cyp3a*$^{-/-}$ treated with vehicle.

2-4. Discussion

A previous report using *Cyp3a*$^{-/-}$ mice has shown that *Cyp3a* deficiency impaired drug metabolism dramatically [15]. We recently showed that hepatic cholesterol and bile acid synthesis were enhanced in the liver of *Cyp3a*$^{-/-}$ mice [66]. Thus, *Cyp3a*$^{-/-}$ mice are useful tools to clarify pharmacological and physiological role of CYP3A *in vivo*.

The results of the present study showed that 6β-hydroxylation activities of testosterone were remarkably decreased in the liver microsomes of *Cyp3a*$^{-/-}$ mice, being consistent with the results of previous studies showing that inactivation of testosterone into 6βHT in the liver is mainly catalyzed by CYP3A [7, 60]. Since the liver is considered to be the most important organ responsible for the catabolism of steroid hormones [13], the *in vitro* findings are consistent with the present *in vivo* results showing that total testosterone levels in the plasma and liver and free testosterone levels in plasma were significantly increased in *Cyp3a*$^{-/-}$ mice (Figs. 12A and 12B). These findings suggest that CYP3A, perhaps hepatic CYP3A, is one of the important determinants that regulate systemic levels of testosterone in mice. In this connection, we showed that total testosterone levels were increased by 1.8 fold and that free levels were increased by 9.0 fold in the plasma of *Cyp3a*$^{-/-}$ mice. This difference appears to come from the different free fractions of testosterone in plasma, which were calculated to be 37% and 7.2% in the plasma of *Cyp3a*$^{-/-}$ and WT mice, respectively. It seemed that binding of testosterone to serum proteins, such as SHBG, is saturated because of the increased levels of testosterone in plasma of *Cyp3a*$^{-/-}$ mice. In any case, the 9.0-fold increase in levels of free testosterone indicates that total clearance of free testosterone was decreased dramatically in *Cyp3a*$^{-/-}$ mice (11% of that in WT mice), suggesting that CYP3A is a major determinant regulating systemic levels of testosterone at least in mice.

Since free testosterone diffuses into a target organ [58], a remarkable increase in free testosterone in plasma is expected to enhance androgen response in target organs including the prostate. In fact, the results of the present study showed testosterone levels and mRNA expression levels of all target genes of the AR examined in this study were significantly increased in the prostates of *Cyp3a*$^{-/-}$ mice (Figs. 12C and 13A). In addition, protein expression levels of SCAP were increased in the prostates of *Cyp3a*$^{-/-}$ mice (Fig. 13B). The results of ChIP assays also showed that specific binding of the AR to the ARE-containing region of the *Sbp* and *Prkcd* promoter [68, 69] was significantly more abundant in the prostates of *Cyp3a*$^{-/-}$ mice than in the prostates of WT mice (Fig. 13C). Furthermore, treatment with bicalutamide to *Cyp3a*$^{-/-}$ mice decreased the mRNA expression levels of AR target genes in the prostates (Fig. 15A). The fold decrease caused by bicalutamide were larger than the fold increase caused by *Cyp3a* deficiency, which implied bicalutamide diminished their physiological and induced expressions regulated by AR in the prostates of *Cyp3a*$^{-/-}$ mice. These findings suggest that androgen response *via* AR activation is stimulated in the prostate of *Cyp3a*$^{-/-}$ mice through the increases of prostatic testosterone levels.

Activated AR has been reported to increase the expression of target genes of SREBP2

involved in cholesterol synthesis and transport through transactivation of SCAP, which enhances maturation of SREBP in LNCaP cells [11, 12]. In accordance with the findings using LNCaP cells, the present study showed that protein expression levels of SCAP and mRNA expression levels of SREBP2 target genes involved in the synthesis and transport of cholesterol were increased in the prostates of *Cyp3a*$^{-/-}$ mice (Figs. 13B and 14B), and they were decreased by bicalutamide treatment to *Cyp3a*$^{-/-}$ mice (Fig. 15B). In addition, expression levels of mature SREBP2 were elevated in the prostates of *Cyp3a*$^{-/-}$ mice (Fig. 14A). Finally, total cholesterol levels were increased in the prostates of *Cyp3a*$^{-/-}$ mice (Fig. 14C). The findings suggest that *Cyp3a* deficiency increases testosterone in plasma and prostates, which enhances cholesterol synthesis *via* the SCAP-SREBP2 pathway in the prostate as reported previously in LNCaP cells [11, 12]. Although high cellular cholesterol levels suppress activation of SREBP2 [31], it seemed that SCAP-mediated activation of SREBP2 exceeded the cholesterol-mediated suppression of SREBP2 in the prostates of *Cyp3a*$^{-/-}$ mice. In addition, it has reported that transcription of *Srd5a2* gene is enhanced by activated SREBP2 [71], suggesting that activated SREBP2 might increase mRNA expression levels of Srd5a2 in the prostates of *Cyp3a*$^{-/-}$ mice.

In this context, we previously reported that SREBP2 was activated in the livers of *Cyp3a*$^{-/-}$ mice, possibly due to impaired synthesis of oxysterols (*e.g.*, 25HC) which can suppress proteolytic activation of SREBP2 [31, 66]. Therefore, the results of this study may imply that the activation of SREBP2 in livers of *Cyp3a*$^{-/-}$ mice is also caused by an increased level of free testosterone. Further study is needed to clarify the impact of AR activation on SREBP2 activation in the livers of *Cyp3a*$^{-/-}$ mice.

The present study showed that *Cyp3a* deficiency dramatically increased free testosterone in plasma, which stimulated androgen response and enhanced cholesterol synthesis in the prostate. Zhang *et al.* [18] reported that altered plasma level of testosterone affects androgen response including physiological development of prostate in castrated mice. However, we could not find any difference in the weight of prostate between *Cyp3a*$^{-/-}$ and WT mice (data not shown). In non-castrated mice, increased testosterone may not induce such physiological effects. On the other hand, this remains possible that increased testosterone and cholesterol levels affect the disease state of the prostate. For example, epidemiological evidence suggested that high levels of circulating testosterone is related to the risk of benign prostate hypertrophy and prostate cancer [72, 73]. In addition, high-fat diets increased the risk of prostate cancer by accumulation of cholesterol [74, 75], whereas cholesterol-lowering drugs (*e.g.*, statins) reduced the risk of advanced prostate cancer [76, 77]. Thus, decreased activity of CYP3A may lead to deterioration of benign prostate hypertrophy and prostate cancer.

In humans, CYP3A4/5, major isoforms of CYP3As in the liver, have variants that reduce the enzyme activities [78, 79]. In addition, Werk *et al.* [80] recently reported the first case of a complete failure of CYP3A enzyme activity due to homozygous loss-of-function mutation of CYP3A4 combined with nonfunctional CYP3A5 [80]. Furthermore, a number of drugs used in clinical settings inhibit CYP3A activity [81]. In particular, drugs including antibacterials, anticancer agents, anti-HIV

agents, antihypertensives, sex steroids and their receptor modulators, and several herbal constituents cause potent and sustained inhibition of CYP3A [82], since they make CYP3A completely nonfunctional until it is replaced with newly synthesized one. Therefore, further studies are needed to clarify the effects of genetic mutations of *CYP3A* genes and treatments with these CYP3A-inhibiting drugs on systemic levels of free testosterone and their potential associations with prostate cancer and benign prostate hypertrophy in humans, as well as in disease model mice such as the transgenic adenocarcinoma of mouse prostate model.

In conclusion, *Cyp3a* deficiency dramatically increased plasma testosterone levels, suggesting that CYP3A is a major determinant regulating systemic levels of testosterone at least in mice. The results also indicated that *Cyp3a* deficiency stimulated androgen response *via* AR activation in the prostate. Finally, *Cyp3a* deficiency increased cholesterogenic gene expression levels and total cholesterol contents in the prostate, which may be caused by activation of the SCAP-SREBP2 pathway.

Conclusions

1. Deficiency of CYP3A enhances hepatic cholesterol synthesis through the activation of SREBP2, which appears to be triggered by the reduction of 25-HC and cholesterol in *Cyp3a*$^{-/-}$ mice.

2. Enhancement of bile acid synthesis from cholesterol seems to be associated with the reduction of cholesterol levels in the livers of *Cyp3a*$^{-/-}$ mice.

3. Deficiency of CYP3A dramatically increased plasma testosterone levels, suggesting that CYP3A is a major determinant regulating systemic levels of testosterone at least in mice.

4. The increased testosterone levels in plasma might raise testosterone levels and activate AR in the prostates of *Cyp3a*$^{-/-}$ mice.

5. Deficiency of CYP3A increased cholesterogenic gene expression levels and total cholesterol contents in the prostate, which may be caused by activation of AR and sequential stimulation of the SCAP-SREBP2 pathway.

References

1. Guengerich, F. P. 1999. Cytochrome P-450 3A4: regulation and role in drug metabolism. *Annu Rev Pharmacol Toxicol* **39**: 1-17.
2. Deb, S., M. Pandey, H. Adomat, and E. S. Guns. 2012. Cytochrome P450 3A-mediated microsomal biotransformation of 1α, 25-dihydroxyvitamin D3 in mouse and human liver: drug-related induction and inhibition of catabolism. *Drug Metab Dispos* **40**: 907-918.
3. Huang, P., B. Zhu, L. S. Wang, D. S. Ouyang, S. L. Huang, X. P. Chen, and H. H. Zhou. 2003. Relationship between CYP3A activity and breast cancer susceptibility in Chinese Han women. *Eur J Clin Pharmacol* **59**: 471-476.
4. Honda, A., G. Salen, Y. Matsuzaki, A. K. Batta, G. Xu, E. Leitersdorf, G. S. Tint, S. K. Erickson, N. Tanaka, and S. Shefer. 2001. Side chain hydroxylations in bile acid biosynthesis catalyzed by CYP3A are markedly up-regulated in Cyp27-/- mice but not in cerebrotendinous xanthomatosis. *J Biol Chem* **276**: 34579-34585.
5. Diczfalusy, U. H. Nylén, P. Elander, and L. Bertilsson. 2011. 4β-Hydroxycholesterol, an endogenous marker of CYP3A4/5 activity in humans. *Br J Clin Pharmacol* **71**: 183-189.
6. Honda, A., T. Miyazaki, J. Ikegami, T. Iwamoto, T. Maeda, Y. Hirayama, T. Saito, T. Teramoto, and Y. Matsuzaki. 2011. Cholesterol 25-hydroxylation activity of CYP3A. *J Lipid Res* **52**: 1509-1516.
7. Waxman, D., J. C. Attisano, F. P. Guengerich, and D. P. Lapenson. 1988. Human liver microsomal steroid metabolism: identification of the major microsomal steroid hormone 6 beta-hydroxylase cytochrome P-450 enzyme. Arch Biochem Biophys **263**: 424-436.
8. Horton, J.D., J. L. Goldstein, and M. S. Brown. 2002. SREBPs: activators of the complete program of cholesterol and fatty acid synthesis in the liver, J Clin Invest **109**: 1125-1131.
9. Radhakrishnan, A., Y. Ikeda, H. J. Kwon, M. S. Brown, and J. L. Goldstein. 2007. Sterol-regulated transport of SREBPs from endoplasmic reticulum to Golgi: oxysterols block transport by binding to Insig. Proc Natl Acad Sci U S A **104**: 6511-6518.
10. Lund, E. G., T. A. Kerr, J. Sakai, W. P. Li, and D. W. Russell. 1998. cDNA cloning of mouse and human cholesterol 25-hydroxylases, polytopic membrane proteins that synthesize a potent oxysterol regulator of lipid metabolism. *J Biol Chem* **273**:34316-34327.
11. Li, X., W. M. Pandak, S. K. Erickson, Y. Ma, L. Yin, P. Hylemon, and S. Ren. 2007. Biosynthesis of the regulatory oxysterol, 5-cholesten-3beta, 25-diol 3-sulfate, in hepatocytes. *J Lipid Res* **48**: 2587-2596.
12. Lund, E., I. Björkhem, C. Furster, and K. Wikvall. 1993. 24-, 25- and 27-hydroxylation of cholesterol by a purified preparation of 27-hydroxylase from pig liver. *Biochim Biophys Acta* **1166**: 177-182.
13. Smith, L. L. 1981. Cholesterol Autoxidation. Plenum. Press, New York.
14. Sar, M., D. B. Lubahn, F. S. French, and E. M. Wilson. 1990. Immunohistochemical localization of the androgen receptor in rat and human tissues, Endocrinology **127**: 3180-3186.

15. Swinnen J. V., W. Ulrix, W. Heyns, and G. Verhoeven. 1997. Coordinate regulation of lipogenic gene expression by androgens: Evidence for a cascade mechanism involving sterol regulatory element binding proteins, Proc. Natl. Acad. Sci. U S A **94**: 12975-12980.
16. Heemers, H., G. Verrijdt, S. Organe, F. Claessens, W. Heyns, G. Verhoeven and J. V. Swinnen. 2004. Identification of an androgen response element in intron 8 of the sterol regulatory element-binding protein cleavage-activating protein gene allowing direct regulation by the androgen receptor, J Biol Chem **279**: 30880-30887.
17. You L. 2004. Steroid hormone biotransformation and xenobiotic induction of hepatic steroid metabolizing enzymes, Chem Biol Interact **147**: 233-246.
18. Zhang, Q. C., Z. Ou, J. H. Lee, M. Xu, U. Kochhar, S. Ren, M. Huang, B. R. Pflug, and W. Xie. 2010. Pregnane X receptor as a therapeutic target to inhibit androgen activity, Endocrinology **151**: 5721-5729.
19. van Herwaarden, A. E. E., E. Wagenaar, C.M. van der Kruijssen, R.A. van Waterschoot, J.W. Smit, J.Y. Song, M.A. van der Valk, O. van Tellingen, J.W. van der Hoorn, H. Rosing, J.H. Beijnen, and A.H. Schinkel. 2007. Knockout of cytochrome P450 3A yields new mouse models for understanding xenobiotic metabolism. J Clin Invest **117**: 3583-3592.
20. Miller, W. L. 1988. Molecular biology of steroid hormone synthesis. *Endocr Rev* **9**: 295-318.
21. Schroepfer, G. J. 2000. Oxysterols: modulators of cholesterol metabolism and other processes. *Physiol Rev* **80**: 361-554.
22. Konrad, B., Benjamin N. Berg, and D. Rittenberg. 1943. The biological conversion of cholesterol to cholic acid. *J. Biol. Chem*. **149**: 511-517.
23. Wiseman, H. 1993. Vitamin D is a membrane antioxidant. Ability to inhibit iron-dependent lipid peroxidation in liposomes compared to cholesterol, ergosterol and tamoxifen and relevance to anticancer action. *FEBS Lett* **326**: 285-288.
24. Brown, M. S., and J. L. Goldstein. 1997. The SREBP pathway: regulation of cholesterol metabolism by proteolysis of a membrane-bound transcription factor. *Cell* **89**: 331-340.
25. Wang, D. Q. 2007. Regulation of intestinal cholesterol absorption. *Annu Rev Physiol* **69**: 221-248.
26. Davis, H. R., L. J. Zhu, L. M. Hoos, G. Tetzloff, M. Maguire, J. Liu, X. Yao, S. P. Iyer, M. H. Lam, E. G. Lund, P. A. Detmers, M. P. Graziano, and S. W. Altmann. 2004. Niemann-Pick C1 Like 1 (NPC1L1) is the intestinal phytosterol and cholesterol transporter and a key modulator of whole-body cholesterol homeostasis. *J Biol Chem* **279**: 33586-33592.
27. Attie, A. D. 2007. ABCA1: at the nexus of cholesterol, HDL and atherosclerosis. *Trends Biochem Sci* **32**: 172-179.
28. Berge, K. E., H. Tian, G. A. Graf, L. Yu, N. V. Grishin, J. Schultz, P. Kwiterovich, B. Shan, R. Barnes, and H. H. Hobbs. 2000. Accumulation of dietary cholesterol in sitosterolemia caused by mutations in adjacent ABC transporters. *Science* **290**: 1771-1775.
29. Wittenburg, H., and M. C. Carey. 2002. Biliary cholesterol secretion by the twinned sterol half-

transporters ABCG5 and ABCG8. *J Clin Invest* **110**: 605-609.
30. Dietschy, J. M., S. D. Turley, and D. K. Spady. 1993. Role of liver in the maintenance of cholesterol and low density lipoprotein homeostasis in different animal species, including humans. *J Lipid Res* **34**: 1637-1659.
31. Russell, D. W. 2003. The enzymes, regulation, and genetics of bile acid synthesis. *Annu Rev Biochem* **72**: 137-174.
32. Bodin, K., U. Andersson, E. Rystedt, E. Ellis, M. Norlin, I. Pikuleva, G. Eggertsen, I. Björkhem, and U. Diczfalusy. 2002. Metabolism of 4 beta -hydroxycholesterol in humans. *J Biol Chem* **277**: 31534-31540.
33. Bodin, K., L. Bretillon, Y. Aden, L. Bertilsson, U. Broomé, C. Einarsson, and U. Diczfalusy. 2001. Antiepileptic drugs increase plasma levels of 4beta-hydroxycholesterol in humans: evidence for involvement of cytochrome p450 3A4. *J Biol Chem* **276**: 38685-38689.
34. Swell, L., C. C. Schwartz, J. Gustafsson, H. Danielsson, and Z. R. Vlahcevic. 1981. A quantitative evaluation of the conversion of 25-hydroxycholesterol to bile acids in man. *Biochim Biophys Acta* **663**: 163-168.
35. Adams, C. M., J. Reitz, J. K. De Brabander, J. D. Feramisco, L. Li, M. S. Brown, and J. L. Goldstein. 2004. Cholesterol and 25-hydroxycholesterol inhibit activation of SREBPs by different mechanisms, both involving SCAP and Insigs. *J Biol Chem* **279**: 52772-52780.
36. Engels, F. K., A. Sparreboom, R. A. Mathot, and J. Verweij. 2005. Potential for improvement of docetaxel-based chemotherapy: a pharmacological review. *Br J Cancer* **93**: 173-177.
37. Kazuki, Y., K. Kobayashi, S. Aueviriyavit, T. Oshima, Y. Kuroiwa, Y. Tsukazaki, N. Senda, H. Kawakami, S. Ohtsuki, S. Abe, M. Takiguchi, H. Hoshiya, N. Kajitani, S. Takehara, K. Kubo, T. Terasaki, K. Chiba, K. Tomizuka, and M. Oshimura. 2013. Trans-chromosomic mice containing a human CYP3A cluster for prediction of xenobiotic metabolism in humans. *Hum Mol Genet* **22**: 578-592.
38. Perloff, M. D., L. L. von Moltke, M. H. Court, T. Kotegawa, R. I. Shader, and D. J. Greenblatt. 2000. Midazolam and triazolam biotransformation in mouse and human liver microsomes: relative contribution of CYP3A and CYP2C isoforms. *J Pharmacol Exp Ther* **292**: 618-628.
39. Bligh, E. G., and W. J. DYER. 1959. A rapid method of total lipid extraction and purification. *Can J Biochem Physiol* **37**: 911-917.
40. Lenicek, M., M. Juklova, J. Zelenka, J. Kovar, M. Lukas, M. Bortlik, and L. Vitek. 2008. Improved HPLC analysis of serum 7alpha-hydroxycholest-4-en-3-one, a marker of bile acid malabsorption. *Clin Chem* **54**: 1087-1088.
41. Dooley, K. A., S. Millinder, and T. F. Osborne. 1998. Sterol regulation of 3-hydroxy-3-methylglutaryl-coenzyme A synthase gene through a direct interaction between sterol regulatory element binding protein and the trimeric CCAAT-binding factor/nuclear factor Y. *J Biol Chem* **273**: 1349-1356.
42. Miettinen, T. A., R. S. Tilvis, and Y. A. Kesäniemi. 1990. Serum plant sterols and cholesterol

precursors reflect cholesterol absorption and synthesis in volunteers of a randomly selected male population. *Am J Epidemiol* **131**: 20-31.

43. Li, T., and J. Y. Chiang. 2005. Mechanism of rifampicin and pregnane X receptor inhibition of human cholesterol 7 alpha-hydroxylase gene transcription. *Am J Physiol Gastrointest Liver Physiol* **288**: G74-84.
44. Ma, Y., and D. Liu. 2012. Activation of pregnane X receptor by pregnenolone 16 α-carbonitrile prevents high-fat diet-induced obesity in AKR/J mice. *PLoS One* **7**: e38734.
45. Spady, D. K., J. A. Cuthbert, M. N. Willard, and R. S. Meidell. 1995. Adenovirus-mediated transfer of a gene encoding cholesterol 7 alpha-hydroxylase into hamsters increases hepatic enzyme activity and reduces plasma total and low density lipoprotein cholesterol. *J Clin Invest* **96**: 700-709.
46. Pullinger, C. R., C. Eng, G. Salen, S. Shefer, A. K. Batta, S. K. Erickson, A. Verhagen, C. R. Rivera, S. J. Mulvihill, M. J. Malloy, and J. P. Kane. 2002. Human cholesterol 7alpha-hydroxylase (CYP7A1) deficiency has a hypercholesterolemic phenotype. *J Clin Invest* **110**: 109-117.
47. Chiang, J. Y., R. Kimmel, and D. Stroup. 2001. Regulation of cholesterol 7alpha-hydroxylase gene (CYP7A1) transcription by the liver orphan receptor (LXRalpha). *Gene* **262**: 257-265.
48. Repa, J. J., K. E. Berge, C. Pomajzl, J. A. Richardson, H. Hobbs, and D. J. Mangelsdorf. 2002. Regulation of ATP-binding cassette sterol transporters ABCG5 and ABCG8 by the liver X receptors alpha and beta. *J Biol Chem* **277**: 18793-18800.
49. Forman, B. M., E. Goode, J. Chen, A. E. Oro, D. J. Bradley, T. Perlmann, D. J. Noonan, L. T. Burka, T. McMorris, W. W. Lamph, R. M. Evans, and C. Weinberger. 1995. Identification of a nuclear receptor that is activated by farnesol metabolites. *Cell* **81**: 687-693.
50. Lu, T. T., M. Makishima, J. J. Repa, K. Schoonjans, T. A. Kerr, J. Auwerx, and D. J. Mangelsdorf. 2000. Molecular basis for feedback regulation of bile acid synthesis by nuclear receptors. *Mol Cell* **6**: 507-515.
51. Nury, T., M. Samadi, A. Varin, T. Lopez, A. Zarrouk, M. Boumhras, J. M. Riedinger, D. Masson, A. Vejux, and G. Lizard. 2013. Biological activities of the LXRα and β agonist, 4β-hydroxycholesterol, and of its isomer, 4α-hydroxycholesterol, on oligodendrocytes: effects on cell growth and viability, oxidative and inflammatory status. *Biochimie* **95**: 518-530.
52. Schwarz, M., E. G. Lund, R. Lathe, I. Björkhem, and D. W. Russell. 1997. Identification and characterization of a mouse oxysterol 7alpha-hydroxylase cDNA. *J Biol Chem* **272**: 23995-24001.
53. Kandutsch, A. A., H. J. Heiniger, and H. W. Chen. 1977. Effects of 25-hydroxycholesterol and 7-ketocholesterol, inhibitors of sterol synthesis, administered orally to mice. *Biochim Biophys Acta* **486**: 260-272.
54. Horton, J. D., I. Shimomura, M. S. Brown, R. E. Hammer, J. L. Goldstein and H. Shimano. 1998. Activation of cholesterol synthesis in preference to fatty acid synthesis in liver and

adipose tissue of transgenic mice overproducing sterol regulatory element-binding protein-2. *J Clin Invest* **101**: 2331-2339.

55. Sonoda, J., L. W. Chong, M. Downes, G. D. Barish, S. Coulter, C. Liddle, C. H. Lee, and R. M. Evans. 2005. Pregnane X receptor prevents hepatorenal toxicity from cholesterol metabolites. Proc Natl Acad Sci U S A **102**: 2198-2203.
56. Hunt, C. M., W. R. Westerkam, G. M. Stave, and J. A. Wilson. 1992. Hepatic cytochrome P-450 3A (CYP3A) activity in the elderly. *Mech Ageing Dev* **64**: 189-199.
57. Inoue, S., K. Yoshinari, M. Sugawara, and Y. Yamazoe. 2011. Activated sterol regulatory element-binding protein-2 suppresses hepatocyte nuclear factor-4-mediated Cyp3a11 expression in mouse liver, Mol Pharmacol **79**: 148-156.
58. Anderson, D. C. 1974. Sex-hormone-binding globulin. *Clin Endocrinol* (Oxf) **3**: 69-96.
59. Mäenpää J, O. Pelkonen, T. Cresteil and A. Rane. 1993. The role of cytochrome P450 3A (CYP3A) isoform(s) in oxidative metabolism of testosterone and benzphetamine in human adult and fetal liver. *The Journal of Steroid Biochemistry and Molecular Biology* **44**: 61-67.
60. Sapone, A., A. Affatato, D. Canistro, M. Broccoli, S. Trespidi, L. Pozzetti, G. L. Biagi, G. Cantelli-Forti, and M. Paolini. 2003. Induction and suppression of cytochrome P450 isoenzymes and generation of oxygen radicals by procymidone in liver, kidney and lung of CD1 mice. *Mutat Res* **527**: 67-80.
61. Draper, A. J., A. Madan, K. Smith and A. Parkinson. 1998. Development of a non-high pressure liquid chromatography assay to determine testosterone hydroxylase (CYP3A) activity in human liver microsomes. *Drug Metab Dispos* **26**: 299-304.
62. Westlind, A., S. Malmebo, I. Johansson, C. Otter, T.B. Andersson, M. Ingelman-Sundberg, and M. Oscarson. 2001. Cloning and tissue distribution of a novel human cytochrome p450 of the CYP3A subfamily, CYP3A43. *Biochem Biophys Res Commun* **281**: 1349-1355.
63. Finnström, N., C. Bjelfman, T. G. Söderström, G. Smith, L. Egevad, B. J. Norlén, C. R. Wolf, and A. Rane. 2001. Detection of cytochrome P450 mRNA transcripts in prostate samples by RT-PCR. *Eur J Clin Invest* **31**: 880-886.
64. Stamey, T. A., J. A. Warrington, M. C. Caldwell, Z. Chen, Z. Fan, M. Mahadevappa, J. E. McNeal, R. Nolley, and Z. Zhang. 2001. Molecular genetic profiling of Gleason grade 4/5 prostate cancers compared to benign prostatic hyperplasia. *J Urol* **166**: 2171-2177.
65. Koch, I., R. Weil, R. Wolbold, J. Brockmöller, E. Hustert, O. Burk, A. Nuessler, P. Neuhaus, M. Eichelbaum, U. Zanger, and L. Wojnowski. 2002. Interindividual variability and tissue-specificity in the expression of cytochrome P450 3A mRNA. *Drug Metab Dispos* **30**: 1108-1114.
66. Hashimoto, M., K. Kobayashi, M. Watanabe, Y. Kazuki, S. Takehara, A. Inaba, S. Nitta, N. Senda, M. Oshimura, and K. Chiba. 2013. Knockout of mouse Cyp3a gene enhances synthesis of cholesterol and bile acid in the liver, *J Lipid Res* **54**: 2060-2068.
67. Yoshimoto, K., H. Echizen, K. Chiba, M. Tani, and T. Ishizaki. 1995. Identification of human

CYP isoforms involved in the metabolism of propranolol enantiomers--N-desisopropylation is mediated mainly by CYP1A2. *Br J Clin Pharmacol* **39**: 421-431.

68. Jariwala, U., J. Prescott, L. Jia, A. Barski, S. Pregizer, J. P. Cogan, A. Arasheben, W.D. Tilley, H.I. Scher, W.L. Gerald, G. Buchanan, G.A. Coetzee, and B. Frenkel. 2007. Identification of novel androgen receptor target genes in prostate cancer. *Mol Cancer* **6**: 39.
69. Viennois, E., T. Esposito, J. Dufour, A. Pommier, S. Fabre, J. L. Kemeny, L. Guy, L. Morel, J. M. Lobaccaro, and S. Baron. 2012. Lxrα regulates the androgen response in prostate epithelium. *Endocrinology* **153**: 3211-3223.
70. Fradet, Y. 2004. Bicalutamide (Casodex) in the treatment of prostate cancer. *Expert Rev Anticancer* Ther **4**: 37-48.
71. Seo, Y., B. Zhu, T. I. Jeon, F. T. Osborne, 2009. Regulation of steroid 5- α reductase type 2 (Srd5a2) by sterol. *Experimental Cell Res*. 315:3133-3139
72. Rannikko, S., and H. Adlercreutz. 1983. Plasma estradiol, free testosterone, sex hormone binding globulin binding capacity, and prolactin in benign prostatic hyperplasia and prostatic cancer. *Prostate* **4**: 223-229.
73. Gann, P. H., C.H. Hennekens, J. Ma, C. Longcope, and M. J. 1996. Stampfer, Prospective study of sex hormone levels and risk of prostate cancer. *J Natl Cancer Inst* **88**: 1118-1126.
74. Solomon, K. R., and M. R. Freeman. 2011. The complex interplay between cholesterol and prostate malignancy. *Urol Clin North Am* **38**: 243-259.
75. Pelton, K., M. R. Freeman, and K. R. Solomon. 2012. Cholesterol and prostate cancer. *Curr Opin Pharmacol* **12**: 751-759.
76. Platz, E. A., M. F. Leitzmann, K. Visvanathan, E. B. Rimm, M. J. Stampfer, W. C. Willett, and E. Giovannucci. 2006. Statin drugs and risk of advanced prostate cancer. *J Natl Cancer Inst* **98:** 1819-1825.
77. Maguire, O., C. Pollock, P. Martin, A. Owen, T. Smyth, D. Doherty, M. J. Campbell, S. McClean, and P. Thompson. 2012. Regulation of CYP3A4 and CYP3A5 expression and modulation of "intracrine" metabolism of androgens in prostate cells by liganded vitamin D receptor. *Mol Cell Endocrinol* **364**: 54-64.
78. Lamba, J. K., Y. S. Lin, E. G. Schuetz, and K. E. Thummel. 2002 Genetic contribution to variable human CYP3A-mediated metabolism. *Adv Drug Deliv Rev* **54**: 1271-1294.
79. Werk, A. N., and I. Cascorbi. 2014. Functional gene variants of CYP3A4. *Clin Pharmacol Ther* **96**: 340-348.
80. Werk, A. N., S. Lefeldt, H. Bruckmueller, G. Hemmrich-Stanisak, A. Franke, M. Roos, C. Küchle, D. Steubl, C. Schmaderer, J.H. Bräsen, U. Heemann, I. Cascorbi, and L. Renders. 2014. Identification and characterization of a defective CYP3A4 genotype in a kidney transplant patient with severely diminished tacrolimus clearance. *Clin Pharmacol Ther* **95**: 416-422.
81. Thummel, K. E., and G. R. Wilkinson. 1998. In vitro and in vivo drug interactions involving human CYP3A. *Annu Rev Pharmacol Toxicol* **38**: 389-430.

82. Zhou, S., S. Yung Chan, B. Cher Goh, E. Chan, W. Duan, M. Huang, and H. L. McLeod, Mechanism-based inhibition of cytochrome P450 3A4 by therapeutic drugs. *Clin Pharmacokinet* **44**: 279-304.

List of publications

This thesis is based on the following publications.

Mari Hashimoto, Kaoru Kobayashi, Mio Watanabe, Yasuhiro Kazuki, Shoko Takehara, Asumi Inaba, Shin-ichiro Nitta, Naoto Senda, Mitsuo Oshimura, Kan Chiba. "Knockout of mouse *Cyp3a* gene enhances synthesis of cholesterol and bile acid in the liver." *Journal of Lipid Research.* 54 (8): 2060 - 2068 (2013).

Mari Hashimoto, Kaoru Kobayashi, Mana Yamazaki, Yasuhiro Kazuki, Shoko Takehara, Mitsuo Oshimura, Kan Chiba, *"Cyp3a* deficiency enhances androgen receptor activity and cholesterol synthesis in the mouse prostate." *J Steroid Biochem Mol Biol*. In press.

Acknowledgements

I would like to show my appreciation to Professor emeritus Kan Chiba who gave me opportunities to do my project work. I thank for his helpful advices and critical review of all of the manuscripts.

I would gratitude to Professor Hidetaka Akita who supervised this thesis. I would like to thank for the many valuable advices.

I wish to express my sincere gratitude to Dr. Kaoru Kobayashi who gave me guidance from the beginning level and discussion for this work. I also appreciate for her encouragement and critical review of the manuscripts.

I would like to show appreciation to Dr. Tomomi Furihata for many beneficial advices, technical supports and fruitful discussion for this work.

I would like to express my gratitude to Professor Mitsuo Oshimura and Dr. Yasuhiro Kazuki for kind donation of *Cyp3a*$^{-/-}$ mice and their cooperation to the completion of my project work.

I would like to express my gratitude to Dr. Naoto Senda and Mr. Shin-ichiro Nitta for their technical supports for this work.

I offer my regards to fellow students and all my friends who support me in any respect during the completion of the project.

Lastly, I wish to thank my parents and sister who inspired, encouraged and fully supported me through my studies.

Reviewers

This work, for the Degree of Doctor of Pharmaceutical Sciences, was examined by the following reviewers who were authorized by Graduate School of Pharmaceutical Sciences, Chiba University.

Chief Reviewer:
Toshihiko Murayama, PhD., Professor of Chiba University
(Graduate School of Pharmaceutical Sciences)

Reviewer:
Itsuko Ishii, PhD., Professor of Chiba University
(Graduate School of Pharmaceutical Sciences)

Reviewer:
Kousei Ito, PhD., Professor of Chiba University
(Graduate School of Pharmaceutical Sciences)